Journal of Medicinal Chemistry Article

J. Med. Chem. **2010,** *53,* 7739–7755 **7739**
DOI: 10.1021/jm100828n

Discovery of Dual Inducible/Neuronal Nitric Oxide Synthase (iNOS/nNOS) Inhibitor Development Candidate 4-((2-Cyclobutyl-1*H*-imidazo[4,5-*b*]pyrazin-1-yl)methyl)-7,8-difluoroquinolin-2(1*H*)-one (KD7332) Part 2: Identification of a Novel, Potent, and Selective Series of Benzimidazole-Quinolinone iNOS/nNOS Dimerization Inhibitors That Are Orally Active in Pain Models

Joseph E. Payne,[†,#,◆] Céline Bonnefous,[†,#,▽] Kent T. Symons,[‡,▼] Phan M. Nguyen,[‡] Marciano Sablad,[§,○] Natasha Rozenkrants,[§,○] Yan Zhang,[§,○] Li Wang,[∥,¶] Nahid Yazdani,[⊥,+] Andrew K. Shiau,[‡,◇] Stewart A. Noble,[†] Peter Rix,[∥,▽] Tadimeti S. Rao,[§,○] Christian A. Hassig,[‡,●] and Nicholas D. Smith*[,†,▽]

[†]*Department of Chemistry,* [‡]*Department of Biology,* [§]*Department of Pharmacology,* [∥]*Department of Drug Metabolism and Pharmacokinetics, and* [⊥]*Department of Analytical Chemistry , Kalypsys, Inc., 10420 Wateridge Circle, San Diego, California 92121.* [#]*These authors contributed equally to this work.* [▽]*Current affiliation: Aragon Pharmaceuticals, San Diego, California 92121.* [○]*Current affiliation: Johnson and Johnson PRD, San Diego, California 92121.* [◆]*Current affiliation: Nitto Denko Technical Corporation, Carlsbad, California 92058.* [¶]*Current affiliation: Bioquant, San Diego, California 92121.* [+]*Current affiliation: Helicon, San Diego, California 92121.* [▼]*Current affiliation: Dart Neuroscience, San Diego, California 92121.* [●]*Current affiliation: Sanford Burnham Research Center, San Diego, California 92121.* [◇]*Current affiliation: Ludwig Cancer Research Center, University of California, San Diego, California 92037*

Received July 3, 2010

Three isoforms of nitric oxide synthase (NOS), dimeric enzymes that catalyze the formation of nitric oxide (NO) from arginine, have been identified. Inappropriate or excessive NO produced by iNOS and/or nNOS is associated with inflammatory and neuropathic pain. Previously, we described the identification of a series of amide-quinolinone iNOS dimerization inhibitors that although potent, suffered from high clearance and limited exposure in vivo. By conformationally restricting the amide of this progenitor series, we describe the identification of a novel series of benzimidazole-quinolinone dual iNOS/nNOS inhibitors with low clearance and sustained exposure in vivo. Compounds were triaged utilizing an LPS challenge assay coupled with mouse and rhesus pharmacokinetics and led to the identification of 4,7-imidazopyrazine **42** as the lead compound. **42** (**KD7332**) (*J. Med. Chem.* **2009**, *52*, 3047−3062) was confirmed as an iNOS dimerization inhibitor and was efficacious in the mouse formalin model of nociception and Chung model of neuropathic pain, without showing tolerance after repeat dosing. Further **42** did not affect motor coordination up to doses of 1000 mg/kg, demonstrating a wide therapeutic margin.

Introduction

Three isoforms of nitric oxide synthase (NOS[a]), dimeric enzymes that catalyze the formation of nitric oxide (NO) from arginine, have been identified.[1] Of the three isoforms, iNOS and nNOS are closely associated with pain. iNOS, which is synthesized in response to inflammatory and immunologic stimuli and is up-regulated following peripheral nerve injury, is implicated in the pathogenesis of numerous diseases including asthma, inflammatory bowel disease, arthritis, and neuropathic pain.[2,3] While NO derived from constitutively expressed nNOS has been shown to augment *N*-methyl-D-aspartate (NMDA) release and is associated with the development of chronic pain,[4] the third isoform, eNOS, is also constitutively expressed and is critical in the maintenance of homeostatic blood pressure, requiring that NOS inhibitor based therapeutics should selectively inhibit the iNOS and/or nNOS isoforms, and not inhibit eNOS.

Drug discovery efforts to date have primarily focused on the development of iNOS selective inhibitors, particularly substrate competitive inhibitors based on the structure of arginine, leading to compounds such as L-NIL (**1**), a nonselective NOS inhibitor (Figure 1).[5] Also related to the structure of arginine, GW271450 (**2**) is an iNOS selective, time-dependent inhibitor that has demonstrated efficacy in preclinical models of pain.[6] However, its close structural similarity to arginine may lead to interference with physiological processes dependent on arginine transport and metabolism.[7] Small molecule inhibitors that are structurally distinct from arginine but that still incorporate a guanidine motif have also been identified. Among these is **3** (AR-C102222),[8] a substrate competitive inhibitor which showed good selectivity for iNOS and was efficacious in a rat adjuvant-induced arthritis model. Inhibitors of iNOS dimerization have also been identified such as **4** (BBS-4),[9] a potent and selective imidazole-based inhibitor that coordinates to the heme iron in the active site of the enzyme. Although, there have been far fewer reports of nNOS selective inhibitors, examples do exist

*To whom correspondence should be addressed. Phone: (858) 754-3481. Fax: (858) 754 3301. E-mail: nsmith@aragonpharm.com. Address: Aragon Pharmaceuticals, Inc., 4215 Sorrento Valley Boulevard, Suite 215, San Diego, California 92121.

[a]Abbreviations: NOS, nitric oxide synthase; NO, nitric oxide; iNOS, inducible NOS; eNOS, endothelial NOS; nNOS, neuronal NOS; hiNOS, human iNOS; miNOS, mouse iNOS; LPS, lipopolysaccharide; SDS-PAGE, sodium dodecyl sulfate polyacrylamide gel electrophoresis; NMDA, *N*-methyl-D-aspartate; DAN, 2,3-diaminonaphthalene; LRMS, low-resolution mass spectra; HRMS, high-resolution mass spectra.

Published on Web 10/08/2010

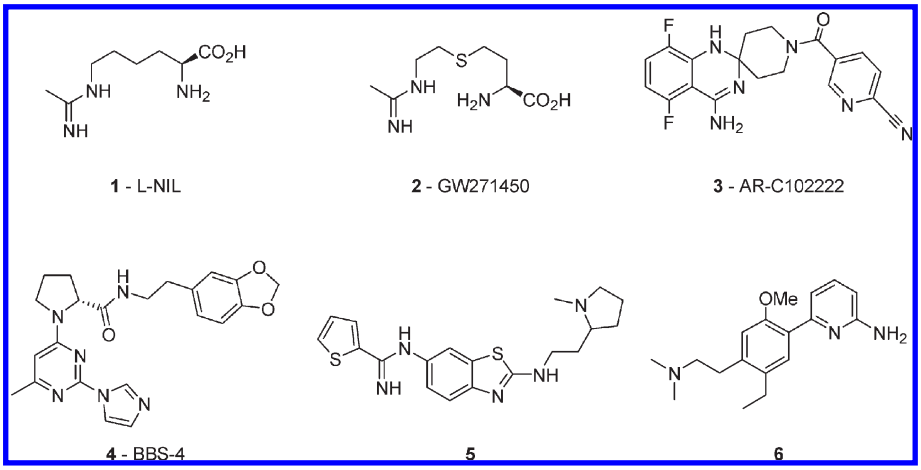

Figure 1. NOS inhibitors.

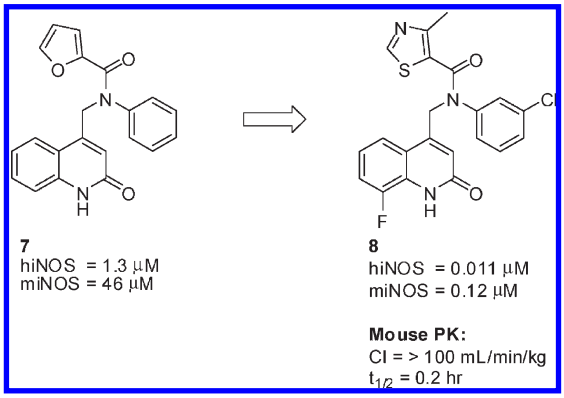

Figure 2. Quinolione iNOS dimerization inhibitor **7**.

such as aminobenzothiazole (**5**)[10] and 2-aminopyridine (**6**),[11] both of which showed good selectivity over eNOS (> 200-fold) and, in the case of **5**, 50-fold selective over iNOS There have been no potent dual iNOS/nNOS inhibitors with good selectivity over eNOS reported to date.

Previously, we described the identification of quinolinone-based iNOS dimerization inhibitor **7** from an ultra high-throughput screen (Figure 2).[12] Optimization of **7** resulted in quinolinone amide **8**, a highly potent human iNOS inhibitor (hiNOS = 0.011 μM), that was > 2000-fold selective over human eNOS. Compound **8** was orally active in a mouse lipopolysaccharide challenge assay measuring plasma nitrates (ED_{50} = 10 mg/kg po) and also in formalin and chronic constriction injury pain models.[12] Although useful as a pharmacological tool, **8** exhibited high clearance (Clp > 100 mL/min/kg) and a short half-life (0.2 h) in mice, which limited exposure and contributed to a short duration of action in these models. We thus sought to evolve the quinolinone amide series to identify potent iNOS selective or dual iNOS/nNOS inhibitors with selectivity over eNOS, but that also had good pharmacokinetics and a suitable drug property profile for development as a neuropathic pain therapeutic.

Toward this end, we looked to remove the amide functionality of **8** and to restrict conformational flexibility by exploring the two new series generated by performing connections "A" and "B" (Figure 3): the "benzimidazole series" (represented by **10**) and the "diaryl series" (represented by **11**).[13] This paper describes the evolution of the benzimidazole series of human iNOS inhibitors to the clinical candidate **42**, 4-((2-cyclobutyl-1*H*-imidazo[4,5-*b*]pyrazin-1-yl)methyl)-7,8-difluoroquinolin-2(1*H*)-one (**KD7332**),[12] a potent dual iNOS/nNOS inhibitor with efficacy in multiple animal pain models. The "diaryl series" represented by **11** will be discussed in separate publication.

Chemistry

The compounds described in this paper were generally prepared by the alkylation of an appropriately substituted benzimidazole core with the bromomethyl quinolinones **57** or **58** (Scheme 1). Synthons **57** and **58** were prepared as follows: keto-amide **53** formed by the reaction of 2-fluoroaniline **51** with methyl 3-oxobutanoate was selectively brominated at the α position[14] to give **55**, which was cyclized under acidic conditions to afford 8-fluoroquinolinone **57** (R_1 = H). The 7,8-difluoroquinolinone **58** was similarly prepared via an analogous sequence. The 2-substituted benzimidazole cores **78**−**98** were prepared under standard condensation conditions from the appropriate carboxylic acid and 1,2-diamionobenzene and then alkylated with either **57** or **58** using NaH/DMF to afford target compounds **10** and **12**−**32**.

Compounds **33**−**36**, **42**, and **44**−**50**, which contain a nitrogen in the six-membered ring of the benzimidazole, were prepared as shown in Scheme 2. Thus cores **104**−**110** were prepared from an appropriately substituted carboxylic acid and a 1,2-diaminoheterocycle, deprotonated (NaH/DMF), and reacted with bromide **58**.[15] However, in contrast to the benzimdazole cores **78**−**98** shown in Scheme 1, the presence of additional ring nitrogens in **104**−**110** meant that there was more than one potential site of alkylation (and hence product regioselectivity). In the case of compound **42**, which has a symmetrical benzimidazole core (X_1 = X_4 = N; X_2 = X_3 = CH), regiochemical assignment was confirmed by the distinctive chemical shift of the quinolinone C3 hydrogen[16] and by NOE experiments. The regiochemistry of the related compounds **44**−**50** were similarly confirmed. The regiochemistry of compounds **33**−**36**, which contain nonsymmetrical benzimidazole cores (X_1 or X_2 or X_3 or X_4 = N), were determined by NOE experiments.

Compounds **37**−**41**, wherein the 7-position of the imidazopyridine was substituted, were prepared as shown in Scheme 3. In the case of the 7-methyl derivative (**37**), commercially available 1,2-diaminopyridine **112** was converted to **113** and then to the final product **37** by employing conditions detailed in Scheme 2. For compounds **39**−**41**, the substituent at the 7-position was installed via displacement of the 7-halopyridine

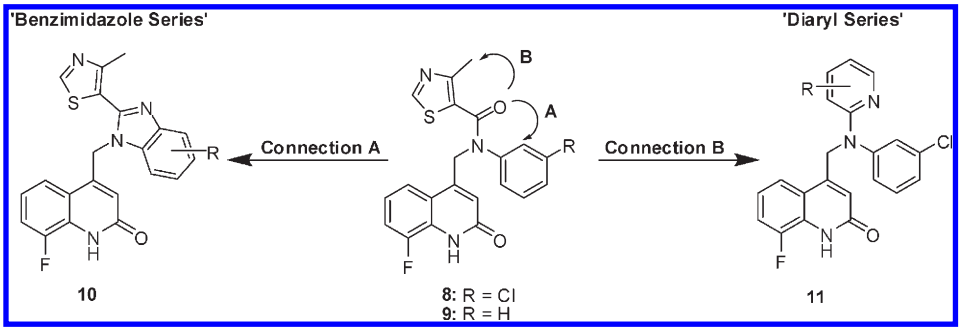

Figure 3. Restricting conformations of the amide of **8** leads to new series.

Scheme 1[a]

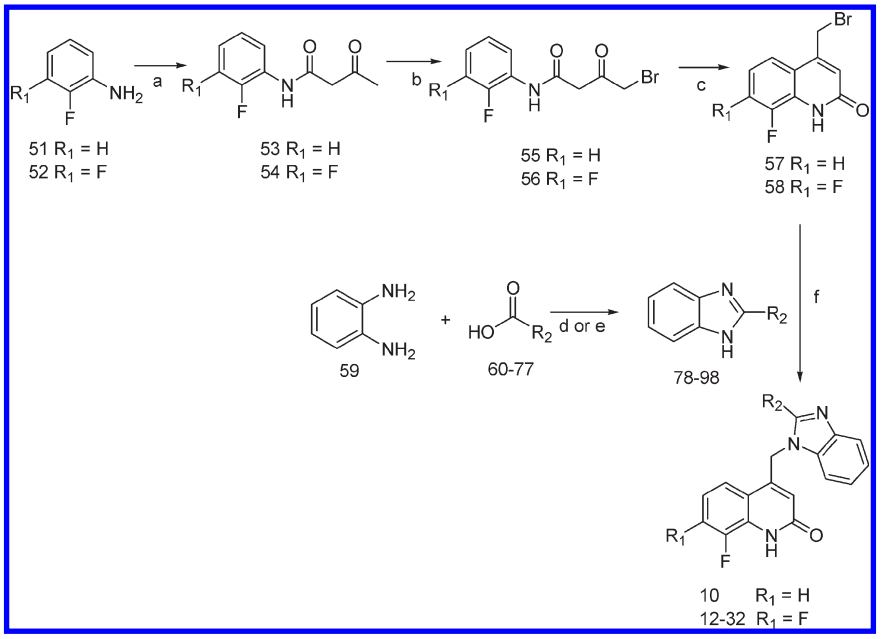

[a] Reagents and conditions: (a) methyl 3-oxobutanoate, pyridine, xylene, reflux, 8.5 h, 38−41% yield; (b) (i) bromine, AcOH, 25 °C, 5 h, (ii) acetone, 25 °C, 18 h, 59−68% yield; (c) H_2SO_4, 45 °C,18 h, 65−89% yield; (d) PPA, 200 °C, 4 h, 21−88% yield; (e) HCl, 100 °C, 18 h, 24−82% yield; (f) NaH, DMF, 25 °C, 1.25 h, 5−83% yield.

Scheme 2[a]

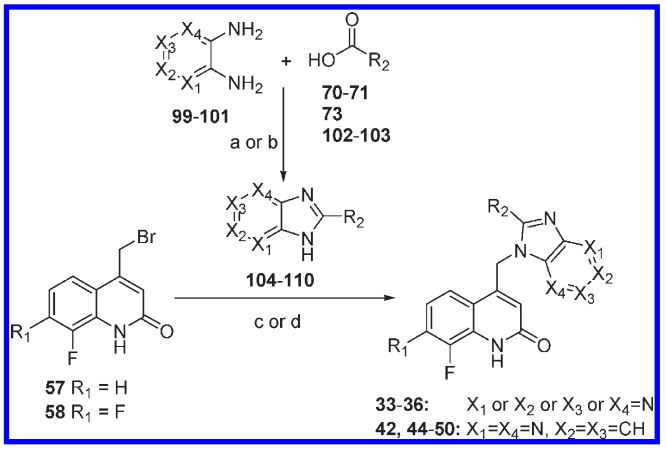

[a] Reagents and conditions: (a) PPA, 100−120 °C, 4 h, 25−90% yield; (b) CDI, ACN, 90 °C, 6 h, 72% yield; (c) NaH, DMF, 25 °C, 1.25 h, 0.5−25% yield; (d) 250 °C, 5 min, 31−75% yield.

intermediates **115** or **116**, followed by alkylation with bromomethyl quinolinone **58**. The 7-chloropyridine intermediate **115** was in turn prepared from pyridine *n*-oxide **114** using $POCl_3$.

As with compound **42**, the regiochemistry of alkylation was confirmed by observing the characteristic chemical shift of the quinolinone C3 hydrogen.[16]

Results and Discussion

Cyclization of amide **9** via connection A (Figure 3) gave benzimidazole **10** (R = H), which resulted in a >10-fold loss in potency (human iNOS EC_{50} = 3.7 μM) and a significant erosion in selectivity over human eNOS (4-fold selective) (Table 1). Additionally, in contrast to amide **9**, benzimidazole **10** was effectively equipotent against human nNOS (hnNOS = 4.3 μM). Previously, we have shown that a 7,8-difluoroquinolinone substitution pattern led to an increase in potency and, as expected, incorporation of this moiety into **10** giving **12** led to an increase in potency (human iNOS EC_{50} = 1.8 μM). Importantly, however, **12** showed a dramatic improvement in mouse microsomal stability compared to **8** (mouse liver microsome $t_{1/2}$ = 98 min versus 9 min)[17] and crucially a corresponding improvement in in vivo clearance (Clp = 12 mL/min/kg versus >100 mL/min/kg) and bioavailability (39%*F* versus 7%*F*) in mice (Table 6). Encouraged by the improvement in mouse pharmacokinetics, we sought to increase the potency and selectivity of this benzimidazole class of NOS inhibitors.

Scheme 3[a]

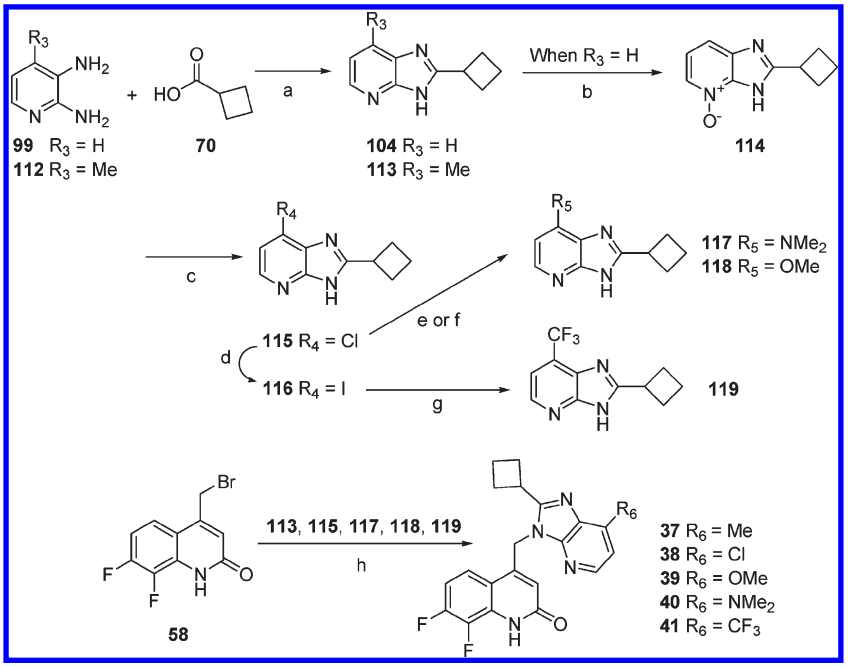

[a] Reagents and conditions: (a) PPA, 100 °C, 4 h, 53−77% yield; (b) mCPBA, acetone, 25 °C, 16 h, 84% yield; (c) $POCl_3$, reflux, 2 h, 75% yield; (d) NaI, TMS-Cl, ACN, reflux, 18 h, 67% yield; (e) dimethylamine, THF, 110 °C, 18 h, 51% yield; (f) sodium methoxide, MeOH, 150 °C, 3 h, 52% yield; (g) KF, CuI, TMSi-CF_3, 55 °C, 18 h, 36% yield; (h) NaH, DMF, 25 °C, 1.25 h, 10−65% yield.

From a SAR perspective, we assumed that the thiazole group of amide **9** mapped onto the thiazole group of benzimidazole **10** (Figure 3) and incorporated groups that had previously been shown to be potent thiazole replacements in the amide series as C-2 benzimidazole substituents (R^2, Table 1). As with the amide series, the *ortho*-methyl substituent on the R^2 ring of **12** was beneficial for potency, as its removal (**13**) reduced potency 5-fold (human iNOS EC_{50} = 8.6 μM). Imidazole **14** and 3-pyridyl **15**, two groups previously shown to be of high potency in the amide series, were also prepared but unexpectedly resulted in reduced iNOS potency (human iNOS EC_{50} > 5 μM), suggesting that simple overlap between the two series could not be assumed. With this in mind, a systematic R^2 pyridine scan was performed (**16**, **17**, **18**), resulting in the demonstration that the 4-pyridyl derivative (**18**) was the more potent inhibitor (human iNOS EC_{50} = 2.2 μM). Incorporation of an *ortho*-methyl substituent on the R^2 ring of **18** gave an increase in potency (**19**: human iNOS EC_{50} = 0.34 μM) similar to that observed for the **13**/**12** pairing. However, further increases in potency (and eNOS selectivity) of the benzimidazole series could not be achieved by R^2 aromatic substitution, although compounds typically had long liver microsomal half-lives, suggesting that the good metabolic stability of **12** was a general characteristic of the benzimidazole scaffold.

Previously, an isopropyl group was shown to be a thiazole replacement in amide **8** (human EC_{50} = 0.16 μM),[12] and so we also examined aliphatic groups at the 2-position of the benzimidazole (Table 2). We were pleased to discover that the isopropyl substituted benzimidazole **20** had submicromolar potency against human iNOS (EC_{50} = 0.80 μM), was equipotent against human nNOS (EC_{50} = 0.65 μM), and was stable in mouse liver microsomes ($t_{1/2}$ > 120 min). Further, when tested in vivo, **20** demonstrated improved mouse pharmacokinetics (Cl = 5.9 mL/min/kg, %F = 58; Table 6) and was efficacious in the mouse LPS challenge assay (ED_{50} = 6 mg/kg po). This result in the LPS challenge assay is noteworthy when comparing the mouse iNOS in vitro potency and in vivo activity of **20** (in vitro mouse EC_{50} = 4.4 μM; LPS ED_{50} = 6 mg/kg po) with that of **8** (in vitro mouse EC_{50} = 0.12 μM; ED_{50} = 10 mg/kg po), clearly illustrating the importance of good pharmacokinetics for robust in vivo activity (Table 6). Despite good mouse PK, **20** was still poorly selective over the human eNOS isoform (14-fold selective), a critical issue that needed to be addressed. The SAR of the R^2 isopropyl substituent was found to be quite sensitive to steric bulk, as truncation to an ethyl group (**21**; human iNOS EC_{50} = 4.3 μM) or expansion to a tertiary butyl group (**22**; human iNOS EC_{50} = 48 μM) led to significant decreases in potency, whereas the simple *n*-propyl substituent maintained activity (**23**; human iNOS EC_{50} = 0.73 μM). Cyclization of the isopropyl group to afford the cyclo-propyl derivative **24** led to a minor loss in potency (human iNOS EC_{50} = 1.6 μM), however upon expansion of the ring size to cyclo-butyl (**25**; human iNOS EC_{50} = 0.26 μM) or cyclo-pentyl (**26**; human iNOS EC_{50} = 0.75 μM), potency improved again. Further increase in ring size to the cyclo-hexyl derivative **27** led to a loss in potency (human iNOS EC_{50} = 8.9 μM), thus demonstrating subtle R^2 size requirements for optimal potency. Of note was the sensitivity of human eNOS potency to changes in the cyclo-alkyl ring size, with cyclo-propyl **24** and cyclo-butyl **25** inhibiting human eNOS at < 10 μM, whereas with a larger ring size, **26** and **27** were effectively noninhibitory (human eNOS > 100 μM). Taken with the human iNOS potency trends, this resulted in improvements in selectivity against human eNOS for **25** (23 fold) and **26** (> 130 fold) compared to **20** (14-fold). Compound **25** also had a long half-life in mouse liver microsomes ($t_{1/2}$ > 120 min) and had good exposure following oral dosing in mouse (C_{max} = 5.7 μg/mL, AUC = 10 μg·h/mL at 10 mg/kg po), which translated into an ED_{50} = 4 mg/kg in the LPS challenge assay. We were able to further exploit the subtle nature of human iNOS/eNOS SAR by preparing the chain extended homologues of **20**, isobutyl derivative **28**, and

Table 1. SAR Examining Heterocycles at the R^2 Position of the Benzimidazole

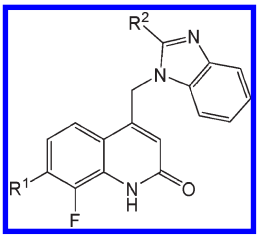

Compd	R^1	R^2	EC_{50} (μM)[a]			Selectivity		Liver Microsome $t_{1/2}$ (min)[b]
			iNOS	eNOS	nNOS	eNOS/iNOS	nNOS/iNOS	
9	NA[c]	NA[c]	0.20 (0.1)	>100[d]	>10[e]	>500	>50	ND[f]
10	H		3.7 (0.40)	15.0 (2.8)	4.3[g]	4.1	1.2	>120
12	F		1.8 (0.15)	6.8 (2.0)	1.5 (0.40)	3.8	0.8	98
13	F		8.6 (2.4)	>100[d]	>10[e]	>12	>12	43
14	F		5.9 (0.5)	5.8 (1.4)	>10[e]	1.0	5.3	>120
15	F		12 (1.0)	>100[d]	>10[e]	>8	>1	>120
16	F		18 (11.4)	>100[d]	>10[e]	>6	>0.5	66
17	F		9.3 (0.6)	>100[d]	>10[e]	>11	>1	>120
18	F		2.2 (0.15)	4.2 (0.4)	2.9 (3.1)	1.9	1.3	64
19	F		0.34 (0.12)	1.3 (0.3)	0.99 (0.27)	3.8	2.9	>120

[a] Cell-based NOS assay using transiently transfected HEK293 cells; NO measured using 2,3-diaminonapthalene (DAN). Each EC_{50} is determined from three separate assay runs, each using a 10-point concentration curve with $n = 8$/point for iNOS and $n = 3$/point for eNOS and nNOS. Standard deviation shown in brackets. [b] Elimination rate under conditions of combined phase I oxidation and phase II glucuronide conjugation (mouse). [c] Not applicable. See Figure 3. [d] < 50% inihition @ 100 μM. [e] < 50% inhibition @ 10 μM (100% being maximal inhibition of control compond **4**). [f] Not determined. [g] $n = 1$ data.

neopentyl derivative **29**. Both **28** and **29** maintained activity against human iNOS ($EC_{50} = 0.38\ \mu M$ and $EC_{50} = 1.36\ \mu M$, respectively) but as with **26** and **27** were highly selective over human eNOS ($EC_{50} > 100\ \mu M$), giving good selectivity ratios (**28**: > 250 fold; **29**: > 70 fold). Preparation of the cyclopropylmethylene **30** further demonstrated the importance of steric bulk for selectivity over human eNOS. Compared to the closely related isopropyl analogue **28**, cyclo-propyl derivative **30** was equipotent against human iNOS ($EC_{50} = 0.60\ \mu M$) but had poor selectivity over human eNOS (human eNOS $EC_{50} = 3.9\ \mu M$; selectivity = 7 fold) compared to > 250-fold selectivity for **28**. Similar to **30**, the cyclobutyl derivative **31** had poor human eNOS selectivity, but expansion of the ring size to cyclo-pentyl (**32**) once again led to more selective human iNOS inhibitors (human eNOS $EC_{50} > 100\ \mu M$) while maintaining potency against human iNOS ($EC_{50} = 1.77\ \mu M$). As with isopropyl derivative **20**, the compounds presented in Table 2 generally had good microsomal half-lives and were equipotent against human nNOS, making them dual iNOS/nNOS inhibitors.

Having shown that careful choice of alkyl substituents at the R^2 position of the benzimidazole could be used to modulate human iNOS potency and selectivity over human eNOS, we next turned to investigate the effect of nitrogen substitution on the benzimidazole core employing the cyclo-butyl derivative **25** as the parent molecule (Table 3).

With the exception of **34** ($X^6 = N$; human iNOS $EC_{50} = 18\ \mu M$), systematic placement of nitrogen at each position of the benzimidazole core was generally tolerated, and in the case of **36** (human iNOS $EC_{50} = 0.18\ \mu M$), a slight increase in potency was observed compared to **25**. As with the alkyl R^2 SAR (Table 2), subtle effects were observed with human eNOS potency, with **33** inhibiting human eNOS with an $EC_{50} = 8.8\ \mu M$ (15-fold selective), while **35** and **36** were effectively inactive on human eNOS ($EC_{50} > 100\ \mu M$), leading to good selectivity for these molecules (> 200-fold selective). With its improved human iNOS potency and good selectivity over human eNOS, imidazopyridine **36** represented an important SAR development. Preliminary SAR on the benzimidazole series (data not shown) had shown that a methyl substituent was tolerated at the 7-position of the benzimidazole, whereas substitution at the 4-, 5- and 6-positions led to a significant loss in human iNOS potency. Thus the 7-position of the benzimidazole was investigated further using imidazopyridine **36** as the core (Table 4).

As illustrated by compounds **37**−**41** (Table 4), although a variety of substituents are tolerated at the 7-position, including electron donating (**39**, **40**) and electron withdrawing (**41**)

Table 2. SAR Examining Aliphatic Groups at the R^2 Position

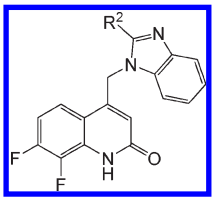

Compd	R^2	EC_{50} (μM)[a]			Selectivity		Liver Microsome $t_{1/2}$ (min)[b]
		iNOS	eNOS	nNOS	eNOS/iNOS	nNOS/iNOS	
20		0.80 (0.14)	11.3 (0.6)	0.65 (0.11)	14	0.8	> 120
21		4.3 (0.9)	1.6 (0.5)	>10[d]	0.4	>2	> 120
22		48 (11)	>100[c]	>100[c]	>2	>2	> 120
23		0.73 (0.1)	1.3 (0.3)	0.69 (0.63)	1.8	0.9	> 120
24		1.6 (0.4)	6.8 (1.0)	1.4 (0.5)	4.3	0.9	> 120
25		0.26 (0.09)	5.9 (2.4)	0.32 (0.12)	23	1.2	> 120
26		0.75 (0.2)	>100[c]	0.77 (0.16)	>133	1.0	> 120
27		8.9 (1.0)	>100[c]	5.0 (1.4)	>11	0.6	> 120
28		0.38 (0.07)	>100[c]	0.69 (0.24)	>263	1.8	110
29		1.36 (0.4)	>100[c]	0.65 (0.82)	>74	0.5	> 120
30		0.60 (0.1)	3.9 (1.0)	0.95 (0.4)	6.5	1.6	> 120
31		0.54 (0.1)	2.9 (0.1)	0.65 (0.22)	5.4	1.2	28
32		1.77 (0.06)	>100[c]	>10[d]	>56	>6	> 120

[a] Cell-based NOS assay using transiently transfected HEK293 cells; NO measured using 2,3-diaminonapthalene (DAN). Each EC_{50} is determined from three separate assay runs, each using a 10-point concentration curve with $n = 8$/point for iNOS and $n = 3$/point for eNOS and nNOS. Standard deviation shown in brackets. [b] Elimination rate under conditions of combined phase I oxidation and phase II glucuronide conjugation (mouse). [c] < 50% inihition @ 100 μM. [d] < 50% inhibition @ 10 μM (100% being maximal inhibition of control compond **4**).

groups, hiNOS potency was not improved relative to **36** (although the compounds do maintain excellent selectivity over eNOS). Further, it was found that these 7-substituted derivatives suffered from limited exposure following oral dosing in mice and corresponding poor performance in the LPS challenge assay (e.g., **40**, AUC = 0.7 μg·h/mL at 10 mg/kg po, Table 6). However, a crucial piece of SAR was discovered by incorporation of a ring nitrogen at the 7-position of **36**, giving symmetrical 4,7-imidazopyrazine **42**. Compound **42** exhibited improved human iNOS potency (human iNOS EC_{50} = 0.091 μM), maintained good selectivity over human eNOS (180 fold selective), was potent against human nNOS (EC_{50} = 0.30 μM), had good mouse pharmacokinetics (Cl = 4.5 mL/min/kg, F = 62%, Table 6) and an excellent ED_{50} in the LPS challenge model (ED_{50} = 1 mg/kg po, Table 6). Further, the symmetrical nature of the imidazopyrazine core of **42** simplified the regioselectivity issues in the synthesis of the other analogues illustrated in Table 4.[18] Having identified this 4,7-imidazopyrazine substitution pattern, we returned to incorporate other potent R^2 alkyl groups on this core (Table 5).

4,7-Imidazopyrazines **42** (human iNOS EC_{50} = 0.091 μM), **44** (human iNOS EC_{50} = 0.28 μM), and **45** (human iNOS EC_{50} = 0.088 μM) demonstrate that human iNOS potency typically improves 3−5-fold when compared to the unsubstituted benzimidazole core (compare to **25**, **26**, **28**: Table 2). An interesting exception to this trend is the isopropyl derivative **46**, which is nearly identical in its in vitro profile to **20** (Table 2). Compound **45**, which is equipotent to **42** against human iNOS but has improved selectivity over human eNOS (440 fold), also had good mouse pharmacokinetics (Cl = 6.1 mL/min/kg; $t_{1/2}$ = 6.0 h ; F = 39%, Table 6) and performed well in the LPS challenge assay (ED_{50} = 0.5 mg/kg po, Table 6).

As described in the Introduction, although a dual human iNOS and nNOS inhibitor was felt to be optimal for efficacy in neuropathic pain models, we also sought to identify human iNOS inhibitors that had selectivity over human nNOS (> 10-fold), both as pharmacological tools but also as potential clinical back-ups. One such compound that showed a modest increase in selectivity over human nNOS was 3,3-difluorocyclobutane **47**, which was potent against human iNOS (EC_{50} = 0.12 μM) and showed a 10-fold selectivity over human nNOS (human nNOS EC_{50} = 1.1 μM). Further increases in selectivity over human nNOS were obtained by applying previously established SAR that showed that compounds that

Table 3. Effect of Nitrogen Substitution on the Benzimidazole Core

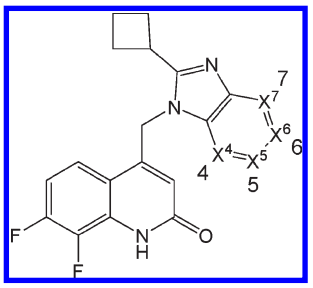

					EC_{50} (μM)[a]			selectivity		
compd	X^7	X^6	X^5	X^4	iNOS	eNOS	nNOS	eNOS/iNOS	nNOS/iNOS	liver microsome $t_{1/2}$ (min)[b]
25	C	C	C	C	0.26 (0.09)	5.9 (2.4)	0.32 (0.12)	23	1.2	> 120
33	N	C	C	C	0.59 (0.1)	8.8 (2.4)	0.52 (0.25)	15	0.9	> 120
34	C	N	C	C	18 (7.8)	21 (3.8)	24 (21)	1.2	1.3	> 120
35	C	C	N	C	0.46(0.2)	> 100[c]	0.73[d]	> 220	1.6	ND[e]
36	C	C	C	N	0.18 (0.01)	> 100[c]	1.3 (0.3)	> 560	7.2	50

[a] Cell-based NOS assay using transiently transfected H EK293 cells; NO measured using 2,3-diaminonapthalene (DAN). Each EC_{50} is determined from three separate assay runs, each using a 10-point concentration curve with $n = 8$/point for iNOS and $n = 3$/point for eNOS and nNOS. Standard deviation shown in brackets. [b] Elimination rate under conditions of combined phase I oxidation and phase II glucuronide conjugation (mouse). [c] < 50% inihition @ 100 μM. [d] $n = 1$ data. [e] Not determined.

Table 4. SAR of Substitution at the 7-Position of the Benzimidazole

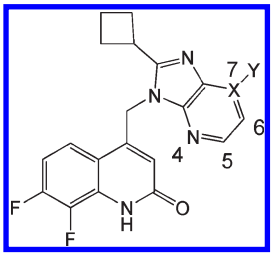

			EC_{50} (μM)[a]			selectivity		
compd	X	Y	iNOS	eNOS	nNOS	eNOS/iNOS	nNOS/iNOS	liver microsome $t_{1/2}$ (min)[b]
36	C	H	0.18 (0.01)	> 100[c]	1.3 (0.3)	> 560	7.2	50
37	C	Me	0.27 (0.04)	> 100[c]	1.6 (0.4)	> 800	12	92
38	C	Cl	0.27 (0.07)	> 100[c]	0.76 (0.3)	> 370	2.8	36
39	C	OMe	0.21 (0.05)	> 100[c]	1.3 (0.1)	> 480	6.2	> 120
40	C	NMe_2	0.17 (0.04)	> 100[c]	1.0 (1.0)	> 590	5.9	8
41	C	CF_3	0.15 (0.06)	> 100[c]	2.0 (1.7)	> 670	13	86
42	N		0.091 (0.01)	16.5 (3.2)	0.30 (0.06)	180	3.3	> 120

[a] Cell-based NOS assay using transiently transfected HEK293 cells; NO measured using 2,3-diaminonapthalene (DAN). Each EC_{50} is determined from three separate assay runs, each using a 10-point concentration curve with $n = 8$/point for iNOS and $n = 3$/point for eNOS and nNOS. Standard deviation shown in brackets. [b] Elimination rate under conditions of combined phase I oxidation and phase II glucuronide conjugation (mouse). [c] < 50% inihition @ 100 μM.

incorporated an 8-fluoroquinolinone had greater selectivity over human nNOS than the 7,8-difluoroquinolinone motif. We thus prepared the 8-fluoroquinolinone derivatives **48**, **49**, and **50**, which although they lost 2−4-fold in human iNOS potency, as predicted had greater selectivity over human nNOS (14−24-fold). Importantly, **48** (Cl = 5.9 mL/min/kg; $F = 91\%$, Table 6) and **50** (Cl = 6.2 mL/min/kg; $F = 55\%$, Table 6) had good mouse PK and were efficacious in the LPS challenge assay with ED_{50}s = 1.5 mg/kg po and 3 mg/kg po, respectively (Table 6).

Having identified potent iNOS inhibitors with good selectivity over eNOS, favorable mouse pharmacokinetics and performance in the LPS challenge assay, we selected **42**, **45**, **48**, and **50** for further profiling in rhesus pharmacokinetics. As shown in Table 7, **42**, **48**, and **50** all had low clearance (4−9 mL/min/kg) and good bioavailability ($\%F = 60-100$) in rhesus monkey, resulting in sustained exposure (AUC@10 mpk ~20 μg·h/mL). A clear exception to this good rhesus pharmacokinetics was **45**, which compared to **42** was of higher clearance (Cl = 18 mL/min/kg) and lower C_{max} (0.21 μg/mL) and AUC (3.2 μg·h/mL). Because of the poorer rhesus pharmacokinetics of **45**, compound **42** was selected as the lead compound for further in vitro characterization and profiling in pharmacology models (vide infra).

Compound **42** was confirmed to disrupt iNOS dimerization by using low-temperature SDS-PAGE to examine the quaternary structure of the iNOS enzyme. As illustrated in Figure 4, treatment with **42** or **4** (an imidazole-based dimerization inhibitor) resulted in loss of dimeric enzyme population, being mechanistically distinct from a substrate competitive inhibitor such as SEITU. These data demonstrate that compound **42**, like its amide

Table 5. Incorporation of Favored R^2 Groups onto the 4,7-Imidazopyrazine Core

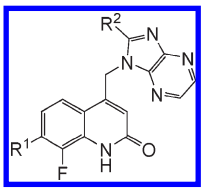

Compd	R^1	R^2	EC_{50} (μM)[a]			Selectivity		Liver Microsome
			iNOS	eNOS	nNOS	eNOS/iNOS	nNOS/iNOS	$t_{1/2}$ (min)[b]
42	F		0.091 (0.01)	17 (3.2)	0.30 (0.06)	180	3.3	>120
44	F		0.28 (0.06)	>100[c]	1.0 (0.3)	>360	3.6	>120
45	F		0.088 (0.01)	39 (9.9)	0.30 (0.02)	440	3.4	47
46	F		0.85 (0.3)	13 (3.8)	0.61 (0.1)	15	0.7	>120
47	F		0.12 (0.01)	9.2 (0.8)	1.1 (0.5)	77	9.2	>120
48	H		0.19 (0.01)	26 (4.9)	4.6 (1.3)	134	24	>120
49	H		0.29 (0.02)	>100[c]	6.8 (3.8)	>350	23	>120
50	H		0.22 (0.05)	>100[c]	3.0 (3.4)	>460	14	>120

[a] Cell-based NOS assay using transiently transfected HEK293 cells; NO measured using 2,3-diaminonapthalene (DAN). Each EC_{50} is determined from three separate assay runs, each using a 10-point concentration curve with $n = 8$/point for iNOS and $n = 3$/point for eNOS and nNOS. Standard deviation shown in brackets. [b] Elimination rate under conditions of combined phase I oxidation and phase II glucuronide conjugation (mouse). [c] < 50% inihition @ 100 μM.

Table 6. Mouse Pharmacokinetics[a] and LPS ED_{50} of Selected Compounds

compd	hiNOS EC_{50} (μM)	miNOS EC_{50} (μM)	Clp (mL/min/kg)	$t_{1/2}$ (h)	Vdss (L/kg)	C_{max} (μg/mL)	AUC (μg·h/mL)	$t_{1/2}$ (hr)[b]	%F	LPS ED_{50} (mg/kg po)
8[c]	0.011 (0.002)	0.12 (0.001)	> 100	0.2	1.6	1.4	0.45	0.9	7	10
12	1.8 (0.15)	10.3 (4.2)	12	2.3	1.2	3.8	5.67	3.1	39	30%[e]
20	0.80 (0.14)	4.4 (1.7)	5.9	2.1	0.7	14	19.3	2.6	58	6
25	0.26 (0.09)	2.1 (0.6)	ND[d]	ND[d]	ND[d]	5.7	10	1.4	ND[d]	4
28	0.38 (0.07)	3.1 (1.3)	12	1.7	1.1	8.7	13.3	5.2	81	85%[e]
40	0.17 (0.04)	1.8 (0.6)	ND[d]	ND[d]	ND[d]	0.4	0.7	1.4	ND[d]	30%[e]
42	0.091 (0.01)	0.43 (0.36)	4.5	2.1	0.39	15	25	2.3	62	1
45	0.088 (0.01)	0.44 (0.1)	6.1	6	6.8	3.7[b]	11	1.8	39	0.5
48	0.19 (0.01)	1.3 (0.7)	5.9	1.3	0.47	15[b]	25	3.1	91	1.5
50	0.22 (0.05)	3.3 (1.4)	6.2	4.0	0.67	8.8	15	2.3	55	3

[a] 3 mg/kg iv; 10 mg/kg po. [b] Per oral $t_{1/2}$. [c] 1 mg/kg iv; 10 mg/kg po. [d] Not determined. [e] % Reduction in nitrate levels compared to vehicle control (compound dosed at 30 mg/kg po).

Table 7. Rhesus Pharmacokinetics of Selected Compounds[a]

compd	Clp (mL/min/kg)	$t_{1/2}$ (h)	Vdss (L/kg)	C_{max} (μg/mL)	AUC (μg·h/mL)	$t_{1/2}$ (h)[b]	%F
42	6.0	13	3.0	3.3	18	9.0	63
45	18	21	19	0.21	3.2	15	59
48	4.3	6.8	1.2	1.8	23	10	93
50	8.6	6.6	1.8	3.4	21	6.1	100

[a] 3 mg/kg iv; 10 mg/kg po. HCl salt. [b] Per oral $t_{1/2}$.

progenitor compound **9**,[12] acts as an iNOS dimerization inhibitor.

Compound **42** was also profiled for off-target activity (Table 8) and did not exhibit any appreciable inhibitory activity against the five major human CYP P450 isoforms or in the hERG patch-clamp assay, with the estimated IC_{50} value for all targets exceeding 30 μM (similarly **45**, **48**, and **50** were also highly selective). The selectivity profile of **42** was also profiled against a panel of 50 targets comprised of G-protein coupled receptors, ion channels, transporters of biogenic

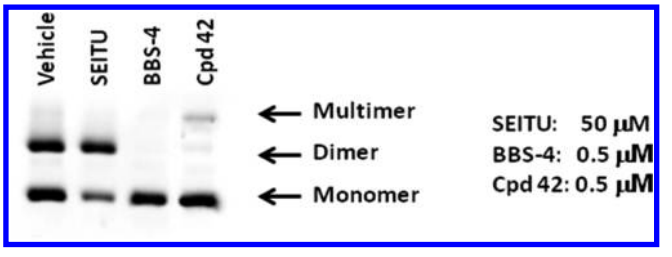

Figure 4. Compound **42** disrupts formation of the iNOS dimer.

Table 8. Cytochrome P450 Inhibition and hERG Values of Selected Compounds

	cytochrome P450 inhibition EC_{50} (μM)					hERG
compd	CYP1A2	CYP3A4	CYP2D6	CYP2C9	CYP2C19	EC_{50} (μM)
42	$>100^a$	$>100^a$	$>100^a$	$>60^a$	$>38^a$	$>30^a$
45	$>100^a$	$>60^a$	$>100^a$	29	$>60^a$	$>30^a$
48	$>100^a$	$>60^a$	$>100^a$	$>60^a$	$>60^a$	$>30^a$
50	35	23	$>100^a$	22	27	NT[b]

[a] < 50% inhibition @ indicated concentration. [b] NT: not tested.

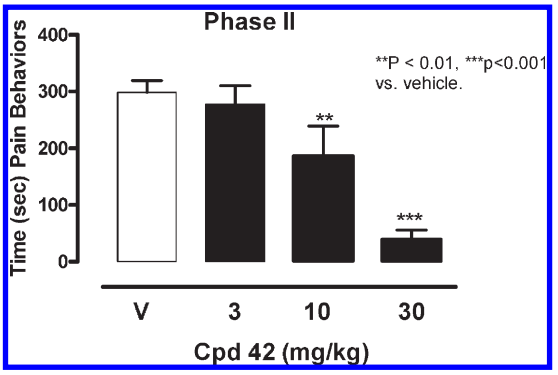

Figure 5. Oral dosing of **42** reduces phase II pain behaviors in the mouse formalin model.

amines, and enzymes (CEREP Screen) at a test concentration of 10 μM. Under these conditions, **42** did not show any measurable interaction at any of the targets examined, indicating that it is remarkably selective and has a unique profile relative to known iNOS inhibitors described in the literature.[2b]

Mouse Models of Pain: Formalin and Spinal Nerve Ligation (Chung) Models. We investigated the ability of compound **42** to reduce pain behaviors in a mouse formalin model of nociceptive pain.[19] Upon injection of formalin into the hind paw, a biphasic pain response was induced. The duration of pain behaviors displayed by the injured paw was then counted, with phase II being from 25 to 45 min postformalin injection. The duration of pain behaviors evoked in phase II are believed to involve the central sensitization of spinal neurons.[20] As can be seen from Figure 5, orally administered **42** gave a dose-responsive attenuation of formalin-induced nocifensive phase II behaviors, with an ED_{50} = 13 mg/kg po.[21] This compared favorably to the corresponding ED_{50} determined for gabapentin in this model (ED_{50} = 110 mg/kg po).[22]

The efficacy of **42** was also assessed in the mouse Chung model of neuropathic pain induced by spinal nerve ligation (Figure 6). In this model, oral dosing of **42** (30 mg/kg) attenuated tactile allodynia to a similar extent as gabapentin at 300 mg/kg.[22] Further, following four days of repeated administration (30 mg/kg BID), the antiallodynic effects of **42** did not show tolerance, which is in contrast to the behavior of morphine, which exhibits rapid tolerance in this model.[22]

We also profiled **42** in a capsaicin-induced thermal hyperalgesia model in rhesus monkeys and demonstrated efficacy in this model. This data and the profiling of compound **42** in additional rodent pain and inflammation models will be presented in a future publication.[22]

Motor Coordination: Rotarod Assay. A number of the currently prescribed neuropathic pain medications have the significant adverse side effect of impairing motor coordination. We thus examined compound **42** for its impact on

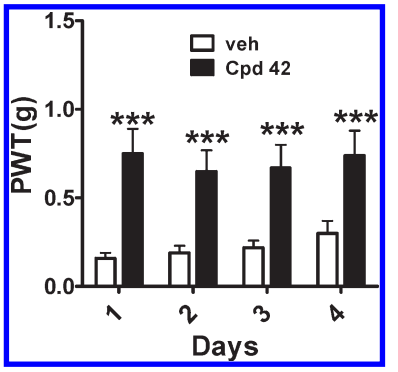

Figure 6. Oral administration of **42** attenuates tactile allodynia in the Chung model without loss of efficacy following repeated administration.

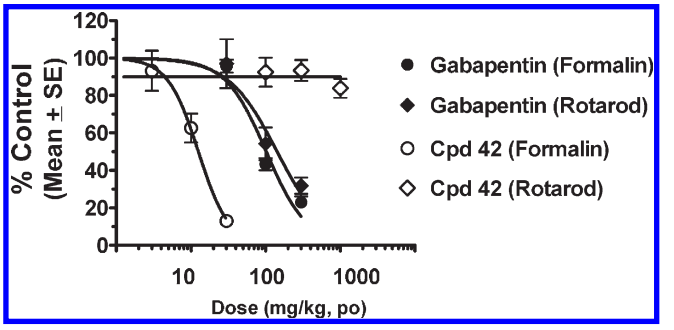

Figure 7. Compound **42** has no measurable impact on motor coordination up to doses of 1000 mg/kg.

motor coordination using the rotarod assay and employing gabapentin as a reference compound. As can be seen from Figure 7, gabapentin adversely impacts motor coordination in mice with a dose−response relationship that effectively overlaps its efficacy profile in the formalin assay. In contrast, compound **42** demonstrated a superior therapeutic window with no measurable impact on rotarod performance (up to a dose of 1000 mg/kg).

Having shown efficacy in a range of neuropathic pain models[22] with a lack of tolerance and side effects, compound **42**, a dual iNOS/nNOS inhibitor with good cross species PK, was nominated as a development progression candidate.

Conclusion

Despite being a potent and selective iNOS inhibitor, the previously described uHTS-derived amide **8** suffered from high in vivo clearance and corresponding poor performance in rodent pain models. By conformationally restricting amide **8**, we identified a novel series of benzimidazole-quinolinone dual iNOS/nNOS inhibitors that demonstrated improved in vivo clearance and sustained exposure following oral dosing. Although initial derivatives suffered from low iNOS potency and poor selectivity over eNOS, SAR studies led to the identification of a 4,7-imidazopyrazine core that greatly improved iNOS potency (and selectivity over eNOS). Compounds were triaged using an LPS challenge assay measuring reduction in plasma nitrates, leading to the identification of a number of potent compounds (LPS ED_{50} < 5 mg/kg po). LPS assay performance coupled with mouse and rhesus PK led to the selection of **42** for further profiling. **42** was confirmed as an iNOS dimerization inhibitor and was found to be highly selective against a panel of off-target receptors, enzymes,

and channels. **42** reduced phase II pain behaviors in a mouse formalin model (ED_{50} = 13 mg/kg) and was efficacious in a mouse Chung model at 30 mg/kg po (compared to gabapentin at 300 mg/kg po), without showing tolerance after repeat dosing. Further, **42** did not impact motor coordination up to doses of 1000 mg/kg, resulting in a wide therapeutic window over beneficial antiallodynic effects. In summary, we have identified development candidate **42**, a potent and selective dual iNOS/nNOS inhibitor with good cross species PK that is efficacious in models of neuropathic pain.

Experimental Section

Chemistry. All reactions were carried out under a nitrogen atmosphere. All solvents and reagents were obtained from commercial sources (unless otherwise specified) and used without further purification. All yields reported are not optimized. Silica gel column chromatography was carried out on either a Jones Chromatography Flashmaster II or an Isco Combiflash Companion XL using prepacked silica gel columns. Reversed-phase semipreparative HPLC purifications were carried out using a Shimadzu Discovery VP system with a SPD-20A prominence UV/vis detector (190−700 nm range). The columns used were either a Waters SunFire C18 (19 mm × 150 mm) or a YMC-Pack Pro ODS-A (20 mm × 150 mm) with a ACN/H_2O solvent mixture stabilized with 0.1% TFA. Proton nuclear magnetic resonances (^{1}H NMR) and carbon nuclear magnetic resonances (^{13}C NMR) were recorded on a Varian 400 MHz Mercury 400VX, and the chemical shifts are reported in parts per million (δ) from an internal standard of residual DMSO (2.50 ppm, 39.5 ppm), methanol (3.31 ppm, 49.0 ppm), or chloroform (7.26 ppm, 77.2 ppm). Proton chemical data are reported as follows: chemical shift, multiplicity (s = singlet, d = doublet, t = triplet, m = multiplet, b = broad), integration, coupling constant. Analytical purity was determined by HPLC and was performed on an Agilent (1100 Series): 1 mg/mL in methanol, 5 μL injection, 254 nm detection, 1 mL/min, 1−95% ACN + 0.05% TFA/H_2O + 0.05% TFA gradient, 15 min. Purity of compounds is >95%. Low-resolution mass spectra (LRMS) were recorded on either a WatersMicromass ZQ or a Waters Acquity (ultra high performance LC) system using electrospray positive ionization. High-resolution mass spectra (HRMS) were obtained on a Waters LCT Premier time-of-flight mass spectrometer using electrospray positive or negative ionization. Exact masses are calculated by MassLynx(c) using the method of calculation based on a published procedure.[23] Melting points were measured on Mettler Toledo FP62 automated melting point apparatus using glass capillary tubes and are uncorrected.

8-Fluoro-4-((2-(4-methylthiazol-5-yl)-1*H*-benzo[*d*]imidazol-1-yl)methyl)quinolin-2(1*H*)-one (10). NaH (60%, 94 mg, 2.34 mmol) was added to a DMF (5 mL) solution of 5-(1*H*-benzo-[d]imidazol-2-yl)-4-methylthiazole (**78**, 219 mg, 1.02 mmol) at 25 °C. After 15 min (end of gas evolution), 4-(bromomethyl)-8-fluoroquinolin-2(1*H*)-one (**57**, 200 mg, 0.78 mmol) was added as a solid to give a brown solution, and the reaction mixture was stirred at 25 °C for 1 h. MeOH was added to quench any unreacted NaH, and the mixture was purified via reverse-phase semipreparative HPLC (ACN:H_2O + 0.1% TFA). The fractions containing the desired compound were combined, and ACN was removed under reduced pressure. Aqueous sodium bicarbonate (50 mL) was added to the aqueous layer, and it was extracted with DCM (3 × 30 mL). The organics were combined, dried, and concentrated under reduced pressure. HCl (4 equiv, 4 M in 1,4-dioxane) was then added, and the resulting mixture was stirred at 25 °C for 1 h, followed by solvent removal under reduced pressure to afford 69 mg (22%) of 8-fluoro-4-((2-(4-methylthiazol-5-yl)-1*H*-benzo[*d*]imidazol-1-yl)methyl)quinolin-2(1*H*)-one (**10**) as an HCl salt. HPLC: t_R = 5.04 (>99%); mp = 289.1 °C. ^{1}H NMR (400 MHz, DMSO-d_6, HCl salt) δ NH resonance not observed, 9.18 (s, 1H), 7.87 (dd, 1H, J = 6.6, 1.2 Hz), 7.72 (dd, 1H, J = 6.4, 1.2 Hz), 7.65 (d, 1H, J = 8.4 Hz), 7.52−7.41 (m, 3H), 7.25 (m, 1H), 5.86 (s, 2H), 5.54 (s, 1H), 2.49 (s, 3H). ^{13}C NMR (400 MHz, DMSO-d_6, HCl salt) δ 161.4, 158.5, 157.8, 149.7 (d, J = 245 Hz, F coupling), 145.7, 145.4, 137.1, 134.7, 128.5, 128.4, 126.0, 125.9, 122.6 (d, J = 7.3 Hz), 120.8, 119.4, 117.7, 117.0 (d, J = 16.8 Hz), 115.1, 113.1, 46.4, 17.2. LRMS (ESI+)/HRMS (ESI−) m/z: calcd for $C_{21}H_{15}FN_4OS$ 391.1, found 391.6 $[M + H]^+$/calcd 389.0873, found 389.0872 $[M - H]^-$.

7,8-Difluoro-4-((2-(4-methylthiazol-5-yl)-1*H*-benzo[*d*]imidazol-1-yl)methyl)quinolin-2(1*H*)-one (12). Compound **12** was synthesized as described for compound **10** using 4-(bromomethyl)-7,8-difluoroquinolin-2(1*H*)-one (**58**) and 5-(1*H*-benzo[*d*]imidazol-2-yl)-4-methylthiazole (**78**) as the starting materials (37% yield). HPLC: t_R = 5.16 (>99%); mp > 300 °C. ^{1}H NMR (400 MHz, DMSO-d_6, HCl salt) δ NH resonance not observed, 9.22 (s, 1H), 7.89 (dd, 1H, J = 8.4, 1.6 Hz), 7.73−7.69 (m, 2H), 7.51−7.44 (m, 2H), 7.36 (m, 1H), 5.88 (s, 2H), 5.55 (s, 1H), 2.50 (s, 3H). ^{13}C NMR (400 MHz, DMSO-d_6, HCl salt) δ 161.6, 157.5, 157.0, 151.1 (dd, J = 247, 9.5 Hz, F coupling), 146.1, 145.8, 139.4, 137.7 (dd, J = 247, 15.3 Hz, F coupling), 135.2, 130.3, 125.4, 125.0, 121.6, 118.8, 118.1, 116.6, 115.7, 112.5, 111.3 (d, J = 18.4 Hz), 45.9, 17.2. LRMS (ESI+)/HRMS (ESI−) m/z: calcd for $C_{21}H_{14}F_2N_4OS$ 409.1, found 409.5 $[M + H]^+$/calcd 407.0778, found 407.0779 $[M - H]^-$.

7,8-Difluoro-4-((2-(thiazol-5-yl)-1*H*-benzo[*d*]imidazol-1-yl)methyl)quinolin-2(1*H*)-one (13). Compound **13** was synthesized as described for compound **10** using 4-(bromomethyl)-7,8-difluoroquinolin-2(1*H*)-one (**58**) and 5-(1*H*-benzo[*d*]imidazol-2-yl)thiazole (**79**) as the starting materials (23% yield). HPLC: t_R = 4.89 (>99%); mp > 300 °C. ^{1}H NMR (400 MHz, DMSO-d_6, HCl salt) δ NH resonance not observed, 9.28 (s, 1H), 8.25 (s, 1H), 7.83−7.80 (m, 2H), 7.69 (d, 1H, J = 6.0 Hz), 7.44−7.36 (m, 3H), 6.10 (s, 2H), 5.31 (s, 1H). ^{13}C NMR (400 MHz, DMSO-d_6, HCl salt) δ 160.9, 158.3, 150.4 (dd, J = 248, 9.5 Hz, F coupling), 145.3, 144.6, 144.0, 139.5, 137.7 (dd, J = 247, 15.0 Hz, F coupling), 135.2, 129.8, 125.3, 124.5, 124.1, 121.0, 118.2, 116.8, 115.0, 111.4, 110.5 (d, J = 19.1 Hz), 45.1. LRMS (ESI+)/HRMS (ESI−) m/z: calcd for $C_{20}H_{12}F_2N_4OS$ 395.1, found 395.2 $[M + H]^+$/calcd 393.0622, found 393.0619 $[M - H]^-$.

7,8-Difluoro-4-((2-(1-methyl-1*H*-imidazol-5-yl)-1*H*-benzo[*d*]-imidazol-1-yl)methyl)quinolin-2(1*H*)-one (14). Compound **14** was synthesized as described for compound **10** using 4-(bromomethyl)-7,8-difluoroquinolin-2(1*H*)-one (**58**) and 2-(1-methyl-1*H*-imidazol-5-yl)-1*H*-benzo[*d*]imidazole (**80**) as the starting materials (10% yield). HPLC: t_R = 4.91 (100%); mp > 300 °C. ^{1}H NMR (400 MHz, DMSO-d_6, HCl salt) δ 12.09 (s, 1H), 9.27 (s, 1H), 7.90−7.86 (m, 2H), 7.70 (m, 1H), 7.63 (m, 1H), 7.43−7.36 (m, 3H), 5.94 (s, 2H), 5.22 (s, 1H), 4.01 (s, 3H). ^{13}C NMR (400 MHz, DMSO-d_6, HCl salt) δ 161.0, 151.1 (dd, J = 247, 9.5 Hz, F coupling), 145.6, 142.0, 140.7, 138.6, 137.7 (dd, J = 247, 15.3 Hz, F coupling), 134.9, 129.8, 124.5, 123.4, 122.2, 121.5, 120.8, 120.0, 116.8, 115.2, 111.4, 110.3 (d, J = 19.0 Hz), 44.6, 35.3. LRMS (ESI+)/HRMS (ESI−) m/z: calcd for $C_{21}H_{15}F_2N_5O$ 392.1, found 392.5 $[M + H]^+$/calcd 390.1167, found 390.1167 $[M - H]^-$.

7,8-Difluoro-4-((2-(4-methylpyridin-3-yl)-1*H*-benzo[*d*]imidazol-1-yl)methyl)quinolin-2(1*H*)-one (15). Compound **15** was synthesized as described for compound **10** using 4-(bromomethyl)-7,8-difluoroquinolin-2(1*H*)-one (**58**) and 2-(4-methylpyridin-3-yl)-1*H*-benzo[*d*]imidazole (**81**) as the starting materials (51% yield). HPLC: t_R = 4.94 (100%); mp = 242.5 °C. ^{1}H NMR (400 MHz, DMSO-d_6, HCl salt) δ NH resonance not observed, 8.88 (s, 1H), 8.78 (d, 1H, J = 6.0 Hz), 7.90 (dd, 1H, J = 6.4, 1.6 Hz), 7.83 (d, 1H, J = 5.6 Hz), 7.71 (d, 1H, J = 7.2 Hz), 7.57 (m, 1H), 7.51−7.44 (m, 2H), 7.29 (m, 1H), 5.82 (s, 2H), 5.64 (s, 1H), 2.42 (s, 3H). ^{13}C NMR (400 MHz, DMSO-d_6, HCl salt) δ 160.8, 154.3, 150.3 (dd, J = 248, 9.0 Hz, F coupling), 147.4, 146.6, 145.3, 144.8, 138.4, 136.8 (dd, J = 247, 15.4 Hz, F coupling), 133.9, 129.5 (d, J = 7.3 Hz), 127.5, 125.0, 124.9, 124.5, 120.9, 118.1, 117.8, 115.0,

112.4, 110.3 (d, J = 18.3 Hz), 45.0, 19.8. LRMS (ESI+)/HRMS (ESI−) m/z: calcd for $C_{23}H_{16}F_2N_4O$ 403.1, found 403.5 $[M + H]^+$/calcd 401.1214, found 401.1211 $[M - H]^-$.

7,8-Difluoro-4-((2-(pyridin-2-yl)-1*H*-benzo[*d*]imidazol-1-yl)methyl)quinolin-2(1*H*)-one (16). Compound **16** was synthesized as described for compound **10** using 4-(bromomethyl)-7,8-difluoroquinolin-2(1*H*)-one (**58**) and 2-(pyridin-2-yl)-1-*H*-benzo[*d*]imidazole (**82**) as the starting materials (8% yield). HPLC: t_R = 5.53 (>94%); mp > 300 °C. ^{1}H NMR (400 MHz, DMSO-d_6, HCl salt) δ NH resonance not observed, 8.48 (d, 1H, J = 4.4 Hz), 8.41 (d, 1H, J = 7.6 Hz), 8.01 (td, 1H, J = 7.8, 2.0 Hz), 7.86 (m, 2H), 7.67 (d, 1H, J = 6.8 Hz), 7.48 (m, 1H), 7.43−7.38 (m, 3H), 6.44 (s, 2H), 5.28 (s, 1H). LRMS (ESI+)/HRMS (ESI−) m/z: calcd for $C_{22}H_{14}F_2N_4O$ 389.1, found 389.5 $[M + H]^+$/calcd 387.1058, found 387.1058 $[M - H]^-$.

7,8-Difluoro-4-((2-(pyridin-3-yl)-1*H*-benzo[*d*]imidazol-1-yl)methyl)quinolin-2(1*H*)-one (17). Compound **17** was synthesized as described for compound **10** using 4-(bromomethyl)-7,8-difluoroquinolin-2(1*H*)-one (**58**) and 2-(pyridin-3-yl)-1*H*-benzo[*d*]imidazole (**83**) as the starting materials (9% yield). HPLC: t_R = 4.63 (100%); mp > 300 °C. ^{1}H NMR (400 MHz, DMSO-d_6, HCl salt) δ NH resonance not observed, 8.99 (d, 1H, J = 2.4 Hz), 8.81 (dd, 1H, J = 5.2, 1.6 Hz), 8.26 (dt, 1H, J = 8.0, 1.8 Hz), 7.91 (d, 1H, J = 7.2 Hz), 7.72−7.67 (m, 3H), 7.52−7.46 (m, 2H), 7.36 (m, 1H), 5.98 (s, 2H), 5.71 (s, 1H). ^{13}C NMR (400 MHz, DMSO-d_6, HCl salt) δ 161.0, 154.3, 150.3 (dd, J = 248, 9.4 Hz, F coupling), 150.3, 149.2, 144.8, 138.7, 136.8 (dd, J = 246, 15.4 Hz, F coupling), 137.2, 134.4, 129.6, 125.1, 124.9, 124.7, 123.4, 120.9, 117.6, 117.5, 115.0, 112.3, 110.4 (d, J = 19.1 Hz), 45.6. LRMS (ESI+)/HRMS (ESI−) m/z: calcd for $C_{22}H_{14}F_2N_4O$ 389.1, found 389.5 $[M + H]^+$/calcd 387.1058, found 387.1059 $[M - H]^-$.

7,8-Difluoro-4-((2-(pyridin-4-yl)-1*H*-benzo[*d*]imidazol-1-yl)methyl)quinolin-2(1*H*)-one (18). Compound **18** was synthesized as described for compound **10** using 4-(bromomethyl)-7,8-difluoroquinolin-2(1*H*)-one (**58**) and 2-(pyridin-4-yl)-1*H*-benzo[*d*]imidazole (**84**) as the starting materials (5% yield). HPLC: t_R = 4.40 (>97%). ^{1}H NMR (400 MHz, DMSO-d_6, HCl salt) δ NH resonance not observed, 8.83 (dd, 2H, J = 4.8, 1.6 Hz), 7.94−7.89 (m, 3H), 7.73 (m, 1H), 7.65 (m, 1H), 7.45−7.39 (m, 3H), 5.99 (s, 2H), 5.49 (s, 1H). LRMS (ESI+)/HRMS (ESI−) m/z: calcd for $C_{22}H_{14}F_2N_4O$ 389.1, found 389.2 $[M + H]^+$/calcd 387.1058 found 387.1056 $[M - H]^-$.

7,8-Difluoro-4-((2-(3-methylpyridin-4-yl)-1*H*-benzo[*d*]imidazol-1-yl)methyl)quinolin-2(1*H*)-one (19). Compound **19** was synthesized as described for compound **10** using 4-(bromomethyl)-7,8-difluoroquinolin-2(1*H*)-one (**58**) and 2-(3-methylpyridin-4-yl)-1*H*-benzo[*d*]imidazole (**85**) as the starting materials (31% yield). HPLC: t_R = 5.14 (>99%); mp = 292.4 °C. ^{1}H NMR (400 MHz, DMSO-d_6, HCl salt) δ NH resonance not observed, 8.97 (s, 1H), 8.77 (d, 1H, J = 6.0 Hz), 7.94−7.90 (m, 2H), 7.68 (m, 1H), 7.58 (m, 1H), 7.48−7.44 (m, 2H), 7.33 (m, 1H), 5.81 (s, 2H), 5.52 (s, 1H), 2.44 (s, 3H). LRMS (ESI+)/HRMS (ESI−) m/z: calcd for $C_{23}H_{16}F_2N_4O$ 403.1, found 403.5 $[M + H]^+$/calcd 401.1214 found 401.1216 $[M - H]^-$.

7,8-Difluoro-4-((2-isopropyl-1*H*-benzo[*d*]imidazol-1-yl)methyl)quinolin-2(1*H*)-one (20). Compound **20** was synthesized as described for compound **10** using 4-(bromomethyl)-7,8-difluoroquinolin-2(1*H*)-one (**58**) and 2-isopropyl-1*H*-benzo[*d*]imidazole (**96**, commercially available) as the starting materials (52% yield). HPLC: t_R = 3.36 (>99%); mp = 262.3 °C. ^{1}H NMR (400 MHz, DMSO-d_6, HCl salt) δ 12.12 (s, 1H), 7.89 (d, 1H, J = 8.0 Hz), 7.80−7.76 (m, 2H), 7.59 (td, 1H, J = 7.6, 0.8 Hz), 7.49 (td, 1H, J = 7.6, 0.8 Hz), 7.45 (m, 1H), 6.14 (s, 2H), 5.52 (s, 1H), 3.62 (m, 1H, J = 6.8 Hz), 1.42 (d, 6H, J = 6.8 Hz). ^{13}C NMR (400 MHz, DMSO-d_6, HCl salt) δ 161.6, 159.9, 151.1 (dd, J = 247, 9.5 Hz, F coupling), 145.1, 137.6 (dd, J = 248, 14.0 Hz, F coupling), 132.5, 132.0, 130.4, 126.8, 126.4, 122.0, 117.5, 115.7, 115.4, 113.6, 111.1 (d, J = 19.1 Hz), 45.5, 26.0, 21.2 (2 carbons). LRMS (ESI+)/HRMS (ESI−) m/z: calcd for $C_{20}H_{17}F_2N_3O$ 354.1, found 354.6 $[M + H]^+$/calcd 352.1262 found 352.1259 $[M - H]^-$.

7,8-Difluoro-4-((2-ethyl-1*H*-benzo[*d*]imidazol-1-yl)methyl)quinolin-2(1*H*)-one (21). Compound **21** was synthesized as described for compound **10** using 4-(bromomethyl)-7,8-difluoroquinolin-2(1*H*)-one (**58**) and 2-ethyl-1*H*-benzo[*d*]imidazole (**97**, commercially available) as the starting materials (62% yield). HPLC: t_R = 3.05 (>98%); mp > 300 °C. ^{1}H NMR (400 MHz, DMSO-d_6, HCl salt) δ 12.19 (s, 1H), 7.91 (d, 1H, J = 8.4 Hz), 7.81 (d, 1H, J = 8.0 Hz), 7.79−7.76 (m, 1H), 7.63−7.55 (m, 2H), 7.47 (m, 1H), 6.11 (s, 2H), 5.60 (s, 1H), 3.20 (q, 2H, J = 7.2 Hz), 1.40 (t, 3H, J = 7.2 Hz). ^{13}C NMR (400 MHz, DMSO-d_6, HCl salt) δ 160.9, 156.3, 150.3 (dd, J = 247, 9.5 Hz, F coupling), 143.9, 136.8 (dd, J = 246, 15.4 Hz, F coupling), 132.0, 131.0, 129.6, 125.9, 125.6, 121.1, 116.9, 115.0, 114.5, 112.7, 110.4 (d, J = 19.1 Hz), 44.5, 18.8, 10.6. LRMS (ESI+)/HRMS (ESI−) m/z: calcd for $C_{19}H_{15}F_2N_3O$ 340.1, found 340.6 $[M + H]^+$/calcd 338.1105 found 338.1109 $[M - H]^-$.

4-((2-*tert*-Butyl-1*H*-benzo[*d*]imidazol-1-yl)methyl)-7,8-difluoroquinolin-2(1*H*)-one (22). Compound **22** was synthesized as described for compound **10** using 4-(bromomethyl)-7,8-difluoroquinolin-2(1*H*)-one (**58**) and 2-*tert*-butyl-1*H*-benzo[*d*]imidazole (**98**, commercially available) as the starting materials (12% yield). HPLC: t_R = 4.19 (>97%); mp > 300 °C. ^{1}H NMR (400 MHz, DMSO-d_6, HCl salt) δ 12.05 (s, 1H), 7.94 (m, 1H), 7.92 (d, 2H, J = 8.4 Hz), 7.63−7.55 (m, 2H), 7.51−7.44 (m, 2H), 6.16 (s, 2H), 5.63 (s, 1H), 1.56 (s, 9H). LRMS (ESI+)/HRMS (ESI−) m/z: calcd for $C_{21}H_19F_2N_3O$ 368.1, found 368.6 $[M + H]^+$/calcd 366.1418 found 366.1418 $[M - H]^-$.

7,8-Difluoro-4-((2-propyl-1*H*-benzo[*d*]imidazol-1-yl)methyl)quinolin-2(1*H*)-one (23). Compound **23** was synthesized as described for compound **10** using 4-(bromomethyl)-7,8-difluoroquinolin-2(1*H*)-one (**58**) and 2-propyl-1*H*-benzo[*d*]imidazole (**86**) as the starting materials (78% yield). HPLC: t_R = 4.00 (>97%); mp > 300 °C. ^{1}H NMR (400 MHz, DMSO-d_6, HCl salt) δ 12.19 (s, 1H), 7.89 (d, 1H, J = 8.0 Hz), 7.78 (m, 2H), 7.61−7.43 (m, 3H), 6.12 (s, 2H), 5.53 (s, 1H), 3.17 (t, 2H, J = 7.2 Hz), 1.85 (sextet, 2H, J = 7.6 Hz), 0.98 (t, 3H, J = 7.2 Hz). ^{13}C NMR (400 MHz, DMSO-d_6, HCl salt) δ 160.9, 155.1, 150.3 (dd, J = 247, 9.5 Hz, F coupling), 144.1, 136.8 (dd, J = 246, 15.4 Hz, F coupling), 132.0, 131.2, 129.5, 125.9, 125.6, 121.1, 116.8, 115.0, 114.6, 112.7, 110.4 (d, J = 18.3 Hz), 44.6, 26.6, 19.8, 13.4. LRMS (ESI+)/HRMS (ESI−) m/z: calcd for $C_{20}H_{17}F_2N_3O$ 354.1, found 354.6 $[M + H]^+$/calcd 352.1262 found 352.1259 $[M - H]^-$.

4-((2-Cyclopropyl-1*H*-benzo[*d*]imidazol-1-yl)methyl)-7,8-difluoroquinolin-2(1*H*)-one (24). Compound **24** was synthesized as described for compound **10** using 4-(bromomethyl)-7,8-difluoroquinolin-2(1*H*)-one (**58**) and 2-cyclopropyl-1*H*-benzo[*d*]imidazole (**87**) as the starting materials (24% yield). HPLC: t_R = 3.76 (>98%); mp = 216 °C (sublimed). ^{1}H NMR (400 MHz, DMSO-d_6, HCl salt) δ 12.05 (s, 1H), 7.80−7.78 (m, 3H), 7.57−7.41 (m, 3H), 6.17 (s, 2H), 5.64 (s, 1H), 2.54 (m, 1H), 1.47 (m, 2H), 1.31 (m, 2H). ^{13}C NMR (400 MHz, DMSO-d_6, HCl salt) δ 160.9, 156.6, 150.3 (dd, J = 247, 9.5 Hz, F coupling), 144.0, 136.8 (dd, J = 246, 15.4 Hz, F coupling), 132.2, 130.9, 129.6, 125.9, 125.3, 121.1, 117.0, 115.1, 114.3, 112.2, 110.5 (d, J = 18.3 Hz), 44.7, 10.3 (2 carbons), 6.5. LRMS (ESI+)/HRMS (ESI−) m/z: calcd for $C_{20}H_{15}F_2N_3O$ 352.1, found 352.6 $[M + H]^+$/calcd 350.1105 found 350.1102 $[M - H]^-$.

4-((2-Cyclobutyl-1*H*-benzo[*d*]imidazol-1-yl)methyl)-7,8-difluoroquinolin-2(1*H*)-one (25). Compound **25** was synthesized as described for compound **10** using 4-(bromomethyl)-7,8-difluoroquinolin-2(1*H*)-one (**58**) and 2-cyclobutyl-1*H*-benzo[*d*]imidazole (**88**) as the starting materials (56% yield). HPLC: t_R = 4.19 (>99%); mp > 300 °C. ^{1}H NMR (400 MHz, DMSO-d_6, HCl salt) δ 12.11 (s, 1H), 7.89 (d, 1H, J = 7.8 Hz), 7.79−7.76 (m, 2H), 7.60−7.42 (m, 3H), 5.99 (s, 2H), 5.53 (s, 1H), 4.15 (quintet, 1H, J = 8.6 Hz), 2.60 (m, 2H), 2.32 (m, 2H), 2.06 (m, 2H). ^{13}C NMR (400 MHz, DMSO-d_6, HCl salt) δ 161.6, 157.5, 151.1 (dd, J = 247,

9.5 Hz, F coupling), 144.9, 137.6 (dd, J = 248, 14.6 Hz, F coupling), 132.8, 132.0, 130.2, 126.6, 126.4, 121.8, 117.6, 115.7, 115.4, 113.3, 111.1 (d, J = 18.3 Hz), 45.3, 30.5, 27.5 (2 carbons), 18.8. LRMS (ESI+)/HRMS (ESI−) m/z: calcd for $C_{21}H_{17}F_2N_3O$ 366.1, found 366.6 $[M + H]^+$/calcd 364.1262 found 364.1258 $[M - H]^-$.

4-((2-Cyclopentyl-1*H*-benzo[*d*]imidazol-1-yl)methyl)-7,8-difluoroquinolin-2(1*H*)-one (26). Compound **26** was synthesized as described for compound **10** using 4-(bromomethyl)-7,8-difluoroquinolin-2(1*H*)-one (**58**) and 2-cyclopentyl-1*H*-benzo[*d*]imidazole (**89**) as the starting materials (36% yield). HPLC: t_R = 4.75 (>99%); mp > 300 °C. ^{1}H NMR (400 MHz, DMSO-d_6, HCl salt) δ 12.11 (s, 1H), 7.89 (d, 1H, J = 8.0 Hz), 7.81−7.77 (m, 2H), 7.58 (t, 1H, J = 7.2 Hz) 7.53−7.43 (m, 2H), 6.14 (s, 2H), 5.53 (s, 1H), 3.68 (quintet, 1H, J = 8.6 Hz), 2.09 (m, 2H), 2.00 (m, 2H), 1.85 (m, 2H), 1.65 (m, 2H). ^{13}C NMR (400 MHz, DMSO-d_6, HCl salt) δ 160.9, 158.3, 150.3 (dd, J = 247, 9.5 Hz, F coupling), 144.4, 136.8 (dd, J = 246, 15.4 Hz, F coupling), 132.0, 131.4, 129.5, 125.9, 125.5, 121.2, 116.8, 115.0, 114.7, 112.7, 110.4 (d, J = 19.0 Hz), 44.7, 35.2, 31.8 (2 carbons), 25.3 (2 carbons). LRMS (ESI+)/HRMS (ESI−) m/z: calcd for $C_{22}H_{19}F_2N_3O$ 380.1, found 380.6 $[M + H]^+$/calcd 378.1418 found 378.1416 $[M - H]^-$.

4-((2-Cyclohexyl-1*H*-benzo[*d*]imidazol-1-yl)methyl)-7,8-difluoroquinolin-2(1*H*)-one (27). Compound **27** was synthesized as described for compound **10** using 4-(bromomethyl)-7,8-difluoroquinolin-2(1*H*)-one (**58**) and 2-cyclohexyl-1*H*-benzo[*d*]imidazole (**90**) as the starting materials (39% yield). HPLC: t_R = 5.24 (>97%); mp > 300 °C. ^{1}H NMR (400 MHz, MSO-d_6, HCl salt) δ 12.15 (s, 1H), 7.90 (d, 1H, J = 7.8 Hz), 7.81 (m, 1H), 7.76 (d, 1H, J = 8.0 Hz), 7.59 (t, 1H, J = 7.6 Hz), 7.54−7.44 (m, 2H), 6.18 (s, 2H), 5.52 (s, 1H), 3.35 (m, 1H), 1.97−1.68 (m, 7H), 1.38−1.24 (m, 3H). ^{13}C NMR (400 MHz, MSO-d_6, HCl salt) δ 160.9, 158.0, 150.3 (dd, J = 247, 9.5 Hz, F coupling), 144.5, 136.8 (dd, J = 248, 15.4 Hz, F coupling), 131.7, 131.3, 129.5, 126.0, 125.6, 121.3, 116.7, 115.0, 114.6, 112.9, 110.4 (d, J = 19.0 Hz), 44.7, 33.9, 30.3 (2 carbons), 24.9 (2 carbons), 24.8. LRMS (ESI+)/HRMS (ESI−) m/z: calcd for $C_{23}H_{21}F_2N_3O$ 394.2, found 394.5 $[M + H]^+$/calcd 392.1575 found 392.1573 $[M - H]^-$.

7,8-Difluoro-4-((2-isobutyl-1*H*-benzo[*d*]imidazol-1-yl)methyl)-quinolin-2(1*H*)-one (28). Compound **28** was synthesized as described for compound **10** using 4-(bromomethyl)-7,8-difluoroquinolin-2(1*H*)-one (**58**) and 2-isobutyl-1*H*-benzo[*d*]imidazole (**91**) as the starting materials (43% yield). HPLC: t_R = 4.55 (>99%); mp > 300 °C. ^{1}H NMR (400 MHz, DMSO-d_6, HCl salt) δ 12.21 (s, 1H), 7.89 (d, 1H, J = 8.0 Hz), 7.80 (m, 1H), 7.75 (d, 1H, J = 8.4 Hz), 7.59 (t, 1H, J = 7.4 Hz), 7.54−7.46 (m, 2H), 6.12 (s, 2H), 5.46 (s, 1H), 3.01 (d, 2H, J = 7.2 Hz), 2.21 (m, 1H), 0.97 (d, 6H, J = 6.8 Hz). ^{13}C NMR (400 MHz, DMSO-d_6, HCl salt) δ 160.8, 154.3, 150.3 (dd, J = 248, 9.2 Hz, F coupling), 144.1, 136.8 (dd, J = 246, 15.4 Hz, F coupling), 131.9, 131.1, 129.6, 126.1, 125.7, 121.3, 116.8, 115.0, 114.6, 112.9, 110.4 (d, J = 18.4 Hz), 44.7, 33.0, 27.0, 21.9 (2 carbons). LRMS (ESI+)/HRMS (ESI−) m/z: calcd for $C_{21}H_{19}F_2N_3O$ 368.1, found 368.6 $[M + H]^+$/calcd 366.1418 found 366.1415 $[M - H]^-$.

7,8-Difluoro-4-((2-isopentyl-1*H*-benzo[*d*]imidazol-1-yl)methyl)-quinolin-2(1*H*)-one (29). Compound **29** was synthesized as described for compound **10** using 4-(bromomethyl)-7,8-difluoroquinolin-2(1*H*)-one (**58**) and 2-isopentyl-1*H*-benzo[*d*]imidazole (**92**) as the starting materials (50% yield). HPLC: t_R = 5.20 (>99%); mp > 300 °C. ^{1}H NMR (400 MHz, DMSO-d_6, HCl salt) δ 12.10 (s, 1H), 7.89 (d, 1H, J = 8.0 Hz), 7.81−7.77 (m, 2H), 7.61−7.43 (m, 3H), 6.12 (s, 2H), 5.53 (s, 1H), 3.16 (t, 2H, J = 7.8 Hz), 1.72 (q, 2H, J = 5.7 Hz), 1.63 (m, 1H), 0.89 (d, 6H, J = 6.4 Hz). ^{13}C NMR (400 MHz, DMSO-d_6, HCl salt) δ 160.8, 155.4, 150.3 (dd, J = 247, 9.5 Hz, F coupling), 144.0, 136.8 (dd, J = 246, 15.4 Hz, F coupling), 131.9, 131.0, 129.6, 125.9, 125.6, 121.2, 116.9, 115.0, 114.6, 112.7, 110.4 (d, J = 19.1 Hz), 44.6, 34.5, 27.1, 23.0, 21.9 (2 carbons). LRMS (ESI+)/HRMS (ESI−) m/z: calcd for $C_{22}H_{21}F_2N_3O$ 382.2, found 382.5 $[M + H]^+$/calcd 380.1575 found 380.1569 $[M - H]^-$.

4-((2-(Cyclopropylmethyl)-1*H*-benzo[*d*]imidazol-1-yl)methyl)-7,8-difluoroquinolin-2(1*H*)-one (30). Compound **30** was synthesized as described for compound **10** using 4-(bromomethyl)-7,8-difluoroquinolin-2(1*H*)-one (**58**) and 2-(cyclopropylmethyl)-1*H*-benzo[*d*]imidazole (**93**) as the starting materials (78% yield). HPLC: t_R = 4.27 (>97%); mp > 300 °C. ^{1}H NMR (400 MHz, DMSO-d_6, HCl salt) δ 12.09 (s, 1H), 7.94 (d, 1H, J = 8.0 Hz), 7.82 (d, 1H, J = 8.0 Hz), 7.78−7.75 (m, 1H), 7.63 (td, 1H, J = 7.6, 0.8 Hz), 7.56 (td, 1H, J = 7.8, 1.2 Hz), 7.48 (m, 1H), 6.13 (s, 2H), 5.52 (s, 1H), 3.16 (d, 2H, J = 7.2 Hz), 1.23 (m, 1H), 0.58 (m, 2H), 0.39 (m, 2H). ^{13}C NMR (400 MHz, DMSO-d_6, HCl salt) δ 160.8, 155.1, 150.3 (dd, J = 248, 9.5 Hz, F coupling), 143.9, 136.8 (dd, J = 247, 15.4 Hz, F coupling), 131.9, 130.9, 129.6, 126.1, 125.8, 121.1, 116.9, 115.0, 114.7, 112.8, 110.4 (d, J = 19.0 Hz), 44.7, 29.2, 7.9, 4.8 (2 carbons). LRMS (ESI+)/HRMS (ESI−) m/z: calcd for $C_{21}H_{17}F_2N_3O$ 366.1, found 366.6 $[M + H]^+$/calcd 364.1262 found 364.1258 $[M - H]^-$.

4-((2-(Cyclobutylmethyl)-1*H*-benzo[*d*]imidazol-1-yl)methyl)-7,8-difluoroquinolin-2(1*H*)-one (31). Compound **31** was synthesized as described for compound **10** using 4-(bromomethyl)-7,8-difluoroquinolin-2(1*H*)-one (**58**) and 2-(cyclobutylmethyl)-1*H*-benzo[*d*]imidazole (**94**) as the starting materials (83% yield). HPLC: t_R = 4.96 (>98%); mp > 300 °C. ^{1}H NMR (400 MHz, DMSO-d_6, HCl salt) δ 12.09 (s, 1H), 7.90 (d, 1H, J = 8.0 Hz), 7.79−7.75 (m, 2H), 7.61 (t, 1H, J = 7.6 Hz), 7.54 (t, 1H, J = 8.4 Hz), 7.48 (m, 1H), 6.13 (s, 2H), 5.44 (s, 1H), 3.34 (d, 2H, J = 7.2 Hz), 2.85 (m, 1H), 2.06 (m, 2H), 1.83 (m, 4H). ^{13}C NMR (400 MHz, DMSO-d_6, HCl salt) δ 160.8, 153.9, 150.3 (dd, J = 247, 9.5 Hz, F coupling), 144.1, 136.8 (dd, J = 246, 15.4 Hz, F coupling), 131.8, 130.9, 129.5, 126.1, 125.7, 121.2, 116.7, 115.0, 114.6, 112.8, 110.4 (d, J = 18.3 Hz), 44.6, 32.4, 31.0, 27.3 (2 carbons), 17.7. LRMS (ESI+)/HRMS (ESI−) m/z: calcd for $C_{22}H_{19}F_2N_3O$ 380.1, found 380.6 $[M + H]^+$/calcd 378.1418 found 378.1413 $[M - H]^-$.

4-((2-(Cyclopentylmethyl)-1*H*-benzo[*d*]imidazol-1-yl)methyl)-7,8-difluoroquinolin-2(1*H*)-one (32). Compound **32** was synthesized as described for compound **10** using 4-(bromomethyl)-7,8-difluoroquinolin-2(1*H*)-one (**58**) and 2-(cyclopentylmethyl)-1*H*-benzo[*d*]imidazole (**95**) as the starting materials (12% yield). HPLC: t_R = 5.42 (>99%); mp > 300 °C. ^{1}H NMR (400 MHz, DMSO-d_6, HCl salt) δ 12.10 (s, 1H), 7.91 (d, 1H, J = 8.0 Hz), 7.81−7.77 (m, 2H), 7.61 (td, 1H, J = 7.6, 0.8 Hz), 7.54 (td, 1H, J = 7.8, 0.8 Hz), 7.48 (m, 1H), 6.15 (s, 2H), 5.45 (s, 1H), 3.24 (d, 2H, J = 8.0 Hz), 2.43 (m, 1H), 1.74 (m, 2H), 1.63 (m, 2H), 1.49 (m, 2H), 1.26 (m, 2H). LRMS (ESI+)/HRMS (ESI−) m/z: calcd for $C_{23}H_{21}F_2N_3O$ 394.2, found 394.6 $[M + H]^+$/calcd 392.1575 found 392.1573 $[M - H]^-$.

4-((2-Cyclobutyl-1*H*-imidazo[4,5-*b*]pyridin-1-yl)methyl)-7,8-difluoroquinolin-2(1*H*)-one (33). Compound **33** was synthesized as the first eluting regioisomer as described for compound **10** using 4-(bromomethyl)-7,8-difluoroquinolin-2(1*H*)-one (**58**) and 2-cyclobutyl-1*H*-imidazo[4,5-*c*]pyridine (**104**) as the starting materials (purification by silica gel column chromatography with a step gradient 4 CVs at 2% MeOH/DCM, followed by 4 CVs at 4% MeOH/DCM) (10% yield). HPLC: t_R = 1.56 (>98%). ^{1}H NMR (400 MHz, DMSO-d_6, HCl salt) δ NH resonance not observed, 8.63 (d, 1H, J = 4.4 Hz), 8.41 (d, 1H, J = 4.0 Hz), 7.80 (m, 1H), 7.65 (dd, 1H, J = 8.0, 5.6 Hz), 7.34 (m, 1H), 5.98 (s, 2H), 5.52 (s, 1H), 4.02 (m, 1H), 2.70−1.98 (m, 6H). The regiochemistry of **33** was determined by NMR spectroscopy measuring nuclear Overhauser effects (NOEs).[24] By irradiating the C-9 methylene, NOEs were observed with the cyclobutyl C-14 methine and the proximal C-13 CH on the pyridine ring.[25] LRMS (ESI+)/HRMS (ESI−) m/z: calcd for $C_{20}H_{16}F_2N_4O$ 367.1, found 367.3 $[M + H]^+$/calcd 365.1214, found 365.1215 $[M - H]^-$.

4-((2-Cyclobutyl-1*H*-imidazo[4,5-*c*]pyridin-1-yl)methyl)-7,8-difluoroquinolin-2(1*H*)-one (34). Compound **34** was synthesized as the first eluting regioisomer as described for compound **10** using 4-(bromomethyl)-7,8-difluoroquinolin-2(1*H*)-one (**58**) and 2-cyclobutyl-1*H*-imidazo[4,5-*c*]pyridine (**105**) as the starting materials

(purification via reverse-phase semipreparative HPLC eluting with ACN:H_2O + 0.1% TFA) (0.5% yield due to the tight separation). HPLC: t_R = 2.17 (>96%). ^{1}H NMR (400 MHz, CD_3OD) δ NH resonance not observed, 9.21 (s, 1H), 8.56 (d, 1H, J = 6.6 Hz), 8.20 (d, 1H, J = 6.6 Hz), 7.79 (m, 1H), 7.34 (m, 1H), 6.00 (s, 2H), 5.42 (s, 1H), 3.91 (m, 1H), 2.67−2.03 (m, 6H). The regiochemistry of **34** was assigned by NMR spectroscopy by measuring nuclear Overhauser effects (NOEs). By irradiating the C-9 methylene, NOEs were observed with the cyclobutyl C-14 methine and the proximal C-13 CH on the pyridine ring, so allowing definitive identification of this signal (δ = 8.20). Further, this C-13 CH is a doublet, suggesting coupling to the C-12 CH (δ = 8.56) and hence the regiochemistry shown.[24] LRMS (ESI+)/HRMS (ESI−) m/z: calcd for $C_{20}H_{16}F_2N_4O$ 367.1, found 367.3 $[M + H]^+$/calcd 365.1214, found 365.1209 $[M - H]^-$.

4-((2-Cyclobutyl-3*H*-imidazo[4,5-*c*]pyridin-3-yl)methyl)-7,8-difluoroquinolin-2(1*H*)-one (35). Compound **35** was synthesized as the second eluting regioisomer as described for compound **10** using 4-(bromomethyl)-7,8-difluoroquinolin-2(1*H*)-one (**58**) and 2-cyclobutyl-1*H*-imidazo[4,5-*c*]pyridine (**105**) as the starting materials (purification by reverse-phase semipreparative HPLC eluting with ACN:H_2O + 0.1% TFA) (0.5% yield due to the tight separation). HPLC: t_R = 2.26 (>99%). ^{1}H NMR (400 MHz, CD_3OD) δ NH resonance not observed, 9.28 (s, 1H), 8.52 (d, 1H, J = 6.0 Hz), 8.03 (d, 1H, J = 6.4 Hz), 7.80 (m, 1H), 7.34 (m, 1H), 5.96 (s, 2H), 5.39 (s, 1H), 3.92 (m, 1H), 2.65−2.01 (m, 6H). The regiochemistry of **35** was assigned by NMR spectroscopy measuring nuclear Overhauser effects (NOEs). By irradiating the C-9 methylene, an NOE were observed with the cyclobutyl C-14 methine. Although we were not able to observe the NOE between the C-9 methylene and the C-13 CH (limited material available), we assigned the stereochemistry shown based on the NOE results for **34**.[23] LRMS (ESI+)/HRMS (ESI−) m/z: calcd for $C_{20}H_{16}F_2N_4O$ 367.1, found 367.3 $[M + H]^+$/calcd 365.1214, found 365.1214 $[M - H]^-$.

4-((2-Cyclobutyl-3*H*-imidazo[4,5-*b*]pyridin-3-yl)methyl)-7,8-difluoroquinolin-2(1*H*)-one (36). Compound **36** was synthesized as the second eluting regioisomer as described for compound **10** using 4-(bromomethyl)-7,8-difluoroquinolin-2(1*H*)-one (**58**) and 2-cyclobutyl-1*H*-imidazo[4,5-*c*]pyridine (**104**) as the starting materials (purification by silica gel column chromatography with a step gradient 4 CVs at 2% MeOH/DCM, followed by 4 CVs at 4% MeOH/DCM) (23% yield). HPLC: t_R = 5.60 (>99%); mp > 300 °C. ^{1}H NMR (400 MHz, DMSO-d_6, HCl salt) δ 8.47 (d, 1H, J = 4.4 Hz), 8.29 (d, 1H, J = 8.0 Hz), 7.83 (m, 1H), 7.53 (m, 1H), 7.39 (m, 1H), 5.84 (s, 2H), 5.60 (s, 1H), 4.09 (m, 1H), 2.60−1.88 (m, 6H). The regiochemistry of **36** was determined by NMR spectroscopy measuring nuclear Overhauser effects (NOEs). By irradiating the C-9 methylene, an NOE was only observed with the cyclobutyl C-14 methine (and not any CH on the pyridine ring as with **33**).[23] ^{13}C NMR (400 MHz, DMSO-d_6) δ 160.9, 158.5, 150.3 (dd, J = 247, 9.5 Hz, F coupling), 145.7, 145.1, 144.6, 136.9 (dd, J = 246, 15.4 Hz, F coupling), 129.5 (d, J = 7.4 Hz), 127.4, 124.6, 120.9, 120.8, 117.4, 115.0, 110.5 (d, J = 18.4 Hz), 42.7, 30.6, 26.6 (2 carbons), 18.0. LRMS (ESI+)/HRMS (ESI−) m/z: calcd for $C_{20}H_{16}F_2N_4O$ 367.1, found 367.3 $[M + H]^+$/calcd 365.1214, found 365.1211 $[M - H]^-$.

4-((2-Cyclobutyl-7-methyl-3*H*-imidazo[4,5-*b*]pyridin-3-yl)methyl)-7,8-difluoroquinolin-2(1*H*)-one (37). Compound **37** was synthesized as described for compound **10** using 4-(bromomethyl)-7,8-difluoroquinolin-2(1*H*)-one (**58**) and 2-cyclobutyl-7-methyl-3*H*-imidazo[4,5-*b*]pyridine (**113**) as the starting materials (12% yield). HPLC: t_R = 4.43 (>99%); mp > 300 °C. ^{1}H NMR (400 MHz, DMSO-d_6) δ 12.02 (s, 1H), 8.13 (d, 1H, J = 4.8 Hz), 7.85 (m, 1H), 7.38 (m, 1H), 7.16 (d, 1H, J = 5.2 Hz), 5.70 (s, 2H), 5.20 (s, 1H), 3.85 (qt, 1H, J = 8.6 Hz), 2.62 (s, 3H), 2.45−1.82 (m, 6H). ^{13}C NMR (400 MHz, DMSO-d_6) δ 160.9, 157.8, 150.3 (dd, J = 247, 9.5 Hz, F coupling), 145.2, 144.8, 136.9, 136.8 (dd, J = 246, 15.4 Hz, F coupling), 129.6, 129.5, 127.8, 121.7, 120.7, 117.2, 115.0, 110.5 (d, J = 19.0 Hz), 42.7, 30.5, 26.9 (2 carbons), 18.0, 16.6. LRMS (ESI+)/HRMS (ESI−) m/z: calcd for $C_{21}H_{18}F_2N_4O$ 381.1, found 381.3 $[M + H]^+$/calcd 379.1371 found 379.1369 $[M - H]^-$.

4-((7-Chloro-2-cyclobutyl-3*H*-imidazo[4,5-*b*]pyridin-3-yl)methyl)-7,8-difluoroquinolin-2(1*H*)-one (38). Compound **38** was synthesized as described for compound **10** using 4-(bromomethyl)-7,8-difluoroquinolin-2(1*H*)-one (**58**) and 7-chloro-2-cyclobutyl-3*H*-imidazo[4,5-*b*]pyridine (**115**) as the starting materials (65% yield). HPLC: t_R = 5.75 (100%). ^{1}H NMR (400 MHz, DMSO-d_6) δ 12.06 (s, 1H), 8.21 (d, 1H, d = 5.2 Hz), 7.82 (m, 1H), 7.44 (d, 1H, J = 5.6 Hz), 7.37 (m, 1H), 5.73 (s, 2H), 5.22 (s, 1H), 3.86 (qt, 1H, J = 8.6 Hz), 2.42−1.82 (m, 6H). LRMS (ESI+)/HRMS (ESI−) m/z: calcd for $C_{20}H_{15}ClF_2N_4O$ 401.1, found 401.2 $[M + H]^+$/calcd 399.0824, found 399.0819 $[M - H]^-$.

4-((2-Cyclobutyl-7-methoxy-3*H*-imidazo[4,5-*b*]pyridin-3-yl)methyl)-7,8-difluoroquinolin-2(1*H*)-one (39). Compound **39** was synthesized as described for compound **10** using 4-(bromomethyl)-7,8-difluoroquinolin-2(1*H*)-one (**58**) and 2-cyclobutyl-7-methoxy-3*H*-imidazo[4,5-*b*]pyridine (**118**) as the starting materials (15% yield). HPLC: t_R = 4.59 (100%). ^{1}H NMR (400 MHz, DMSO-d_6; TFA salt) δ NH resonance not observed, 8.05 (d, 1H, J = 4.6 Hz), 7.65 (m, 1H), 7.21 (m, 1H), 6.82 (d, 1H, J = 4.4 Hz), 5.58 (s, 2H), 5.11 (s, 1H), 3.90 (s, 3H), 3.68 (m, 1H), 2.43−1.62 (m, 6H). LRMS (ESI+)/HRMS (ESI+) m/z: calcd for $C_{21}H_{18}F_2N_4O_2$ 397.1, found 397.3 $[M + H]^+$/calcd 397.1476, found 397.1475 $[M + H]^+$.

4-((2-Cyclobutyl-7-(dimethylamino)-3*H*-imidazo[4,5-*b*]pyridin-3-yl)methyl)-7,8-difluoroquinolin-2(1*H*)-one (40). Compound **40** was synthesized as described for compound **10** using 4-(bromomethyl)-7,8-difluoroquinolin-2(1*H*)-one (**58**) and 2-cyclobutyl-*N*,*N*-dimethyl-3*H*-imidazo[4,5-*b*]pyridin-7-amine (**117**) as the starting materials (10% yield). HPLC: t_R = 5.33 (>97%). ^{1}H NMR (400 MHz, DMSO-d_6; TFA salt) δ 12.09 (s, 1H), 7.95 (d, 1H, J = 7.2 Hz), 7.75 (m, 1H), 7.41 (m, 1H), 6.59 (d, 1H, J = 6.8 Hz), 5.69 (s, 2H), 5.15 (s, 1H), 3.77 (qt, 1H, J = 8.4 Hz), 3.55 (s, 6H), 2.40−1.86 (m, 6H). LRMS (ESI+)/HRMS (ESI−) m/z: calcd for $C_{22}H_{21}F_2N_5O$ 410.2, found 410.5 $[M + H]^+$/calcd 408.1636, found 408.1638 $[M - H]^-$.

4-((2-Cyclobutyl-7-(trifluoromethyl)-3*H*-imidazo[4,5-*b*]pyridin-3-yl)methyl)-7,8-difluoroquinolin-2(1*H*)-one (41). Compound **41** was synthesized as described for compound **10** using 4-(bromomethyl)-7,8-difluoroquinolin-2(1*H*)-one (**58**) and 2-cyclobutyl-7-(trifluoromethyl)-3*H*-imidazo[4,5-*b*]pyridine (**119**) as the starting materials (55% yield). HPLC: t_R = 6.19 (100%). ^{1}H NMR (400 MHz, DMSO-d_6) δ NH resonance not observed, 8.46 (d, 1H, J = 4.8 Hz), 7.83 (m, 1H), 7.62 (d, 1H, J = 5.2 Hz), 7.39 (m, 1H), 5.78 (s, 2H), 5.22 (s, 1H), 3.91 (qt, 1H, J = 8.4 Hz), 2.45−1.88 (m, 6H). LRMS (ESI+)/HRMS (ESI−) m/z: calcd for $C_{21}H_{15}F_5N_4O$ 435.2, found 435.2 $[M + H]^+$/calcd 433.1088, found 433.1090 $[M - H]^-$.

4-((2-Cyclobutyl-1*H*-imidazo[4,5-*b*]pyrazin-1-yl)methyl)-7,8-difluoroquinolin-2(1*H*)-one (42). Compound **42** was synthesized as described for compound **10** using 4-(bromomethyl)-7,8-difluoroquinolin-2(1*H*)-one (**58**) and 2-cyclobutyl-1*H*-imidazo[4,5-*b*]pyrazine (**106**) as the starting materials (25% yield). HPLC: t_R = 5.29 (>99%); mp = 261 °C. ^{1}H NMR (400 MHz, DMSO-d_6; HCl salt) δ 8.53 (d, 1H), 8.33 (d, 1H), 7.83 (m, 1H), 7.40 (m, 1H), 5.78 (s, 2H), 5.36 (s, 1H), 3.95 (m, 1H), 2.5−1.8 (m, 6H). ^{13}C NMR (400 MHz, DMSO-d_6, citrate salt) δ 163.0, 160.9, 150.3 (dd, J = 247, 9.5 Hz, F coupling), 148.3, 145.6, 140.8, 139.5, 137.7, 136.9 (dd, J = 246, 15.4 Hz, F coupling), 129.6 (d, J = 8.1 Hz), 120.7, 117.1, 115.1, 110.5 (d, J = 18.3 Hz), 42.0, 31.6, 26.6 (2 carbons), 18.0. LRMS (ESI+)/HRMS (ESI−) m/z: calcd for $C_{19}H_{15}F_2N_5O$ 368.1, found 368.2 $[M + H]^+$/calcd 366.1167, found 366.1170 $[M - H]^-$.

The minor regioisomer (**43**), 4-((2-cyclobutyl-4*H*-imidazo[4,5-*b*]pyrazin-4-yl)methyl)-7,8-difluoroquinolin-2(1*H*)-one), was also isolated. ^{1}H NMR (400 MHz, DMSO-d_6) δ NH resonance not observed, 8.85 (d, 1H, J = 4.4 Hz), 8.76 (d, 1H, J = 4.0 Hz),

7.84 (m, 1H), 7.37 (m, 1H), 6.32 (s, 2H), 6.26 (s, 1H), 4.01 (m, 1H), 2.55−1.95 (m, 6H).

4-((2-Cyclopentyl-1*H*-imidazo[4,5-*b*]pyrazin-1-yl)methyl)-7,8-difluoroquinolin-2(1*H*)-one (44). Compound **44** was synthesized as described for compound **10** using 4-(bromomethyl)-7,8-difluoroquinolin-2(1*H*)-one (**58**) and 2-cyclopentyl-1*H*-imidazo[4,5-*b*]pyrazine (**107**) as the starting materials (23% yield). HPLC: t_R = 5.39 (>97%); mp = 277.4 °C. ^{1}H NMR (400 MHz, DMSO-d_6) δ NH resonance not observed, 8.49 (d, 1H, J = 2.8 Hz), 8.30 (d, 1H, J = 2.8 Hz), 7.84 (m, 1H), 7.39 (m, 1H), 5.86 (s, 2H), 5.33 (s, 1H), 3.46 (qt, 1H, J = 8.0 Hz), 2.01−1.58 (m, 8H). ^{13}C NMR (400 MHz, DMSO-d_6) δ 164.6, 160.9, 150.3 (dd, J = 247, 9.6 Hz, F coupling), 147.6, 145.6, 140.4, 139.7, 137.9, 136.9 (dd, J = 246, 15.4 Hz, F coupling), 129.6 (d, J = 9.0 Hz), 120.8, 117.1, 115.1, 110.5 (d, J = 19.1 Hz), 42.2, 36.5, 31.9 (2 carbons), 25.5 (2 carbons). LRMS (ESI+)/HRMS (ESI−) m/z: calcd for $C_{20}H_{17}F_2N_5O$ 382.1, found 382.3 $[M + H]^+$/calcd 380.1323, found 380.1326 $[M - H]^-$.

7,8-Difluoro-4-((2-isobutyl-1*H*-imidazo[4,5-*b*]pyrazin-1-yl)-methyl)quinolin-2(1*H*)-one (45). Compound **45** was synthesized as described for compound **10** using 4-(bromomethyl)-7,8-difluoroquinolin-2(1*H*)-one (**58**) and 2-isobutyl-1*H*-imidazo[4,5-*b*]pyrazine (**108**) as the starting materials (20% yield). HPLC: t_R = 5.12 (100%). ^{1}H NMR (400 MHz, DMSO-d_6) δ 12.08 (s, 1H), 8.50 (d, 1H, J = 2.4 Hz), 8.31 (d, 1H, J = 2.8 Hz), 7.83 (m, 1H), 7.38 (m, 1H), 5.85 (s, 2H), 5.31 (s, 1H), 2.85 (d, 2H, J = 6.8 Hz), 2.26 (qt, 1H, J = 7.0 Hz), 0.95 (d, 6H, J = 6.8 Hz). ^{13}C NMR (400 MHz, DMSO-d_6) δ 160.9, 160.2, 150.4 (dd, J = 247, 9.6 Hz, F coupling), 148.3, 145.5, 140.4, 139.6, 137.7, 137.0 (dd, J = 247, 14.8 Hz, F coupling), 129.6 (d, J = 9.0 Hz), 120.8, 117.0, 115.2, 110.5 (d, J = 19.1 Hz), 42.1, 35.5, 26.6, 22.2 (2 carbons). LRMS (ESI+)/HRMS (ESI−) m/z: calcd for $C_{19}H_{17}F_2N_5O$ 370.1, found 370.3 $[M + H]^+$/calcd 368.1323, found 368.1318 $[M - H]^-$.

7,8-Difluoro-4-((2-isopropyl-1*H*-imidazo[4,5-*b*]pyrazin-1-yl)-methyl)quinolin-2(1*H*)-one (46). Compound **46** was synthesized as described for compound **10** using 4-(bromomethyl)-7,8-difluoroquinolin-2(1*H*)-one (**58**) and 2-isopropyl-1*H*-imidazo[4,5-*b*]pyrazine (**109**) as the starting materials (18% yield). HPLC: t_R = 4.48 (100%). ^{1}H NMR (400 MHz, DMSO-d_6) δ 12.10 (s, 1H), 8.49 (d, 1H, J = 2.8 Hz), 8.30 (d, 1H, J = 2.4 Hz), 7.83 (m, 1H), 7.37 (m, 1H), 5.86 (s, 2H), 5.32 (s, 1H), 3.31 (qt, 1H, J = 6.8 Hz), 1.31 (d, 6H, J = 6.8 Hz). ^{13}C NMR (400 MHz, DMSO-d_6) δ 165.4, 160.9, 150.4 (dd, J = 247, 9.6 Hz, F coupling), 148.3, 145.8, 140.4, 139.7, 137.8, 137.0 (dd, J = 246, 14.6 Hz, F coupling), 129.6 (d, J = 9.0 Hz), 120.8, 117.0, 115.2, 110.6 (d, J = 18.3 Hz), 42.1, 26.4, 21.3 (2 carbons). LRMS (ESI+)/HRMS (ESI−) m/z: calcd for $C_{18}H_{15}F_2N_5O$ 356.1, found 356.2 $[M + H]^+$/calcd 354.1167, found 354.1161 $[M - H]^-$.

4-((2-(3,3-Difluorocyclobutyl)-1*H*-imidazo[4,5-*b*]pyrazin-1-yl)-methyl)-7,8-difluoroquinolin-2(1*H*)-one (47). A mixture of 2-(3,3-difluorocyclobutyl)-1*H*-imidazo[4,5-*b*]pyrazine (**110**, 115 mg, 0.54 mmol) and 4-(bromomethyl)-7,8-difluoroquinolin-2(1*H*)-one (**58**, 50 mg, 0.18 mmol) were combined into a 4 mL vial, stirred with a spatula for 1 min, and heated in a sand bath at 250 °C for 5 min. During this time, the powdered mixture congealed, darkened, and melted. After cooling to 25 °C, the crude solid was taken up in DMSO and purified via reverse-phase semipreparative HPLC (ACN:H_2O + 0.1% TFA) to afford 35 mg (48%) of 4-((2-(3,3-difluorocyclobutyl)-1*H*-imidazo[4,5-*b*]pyrazin-1-yl)-methyl)-7,8-difluoroquinolin-2(1*H*)-one. HPLC: t_R = 4.78 (>93%); mp > 300 °C. ^{1}H NMR (400 MHz, DMSO-d_6; HCl salt) δ NH resonance not observed, 8.54 (d, 1H, J = 2.4 Hz), 8.34 (d, 1H, J = 2.8 Hz), 7.80 (m, 1H), 7.38 (m,1H), 5.81 (s, 2H), 5.42 (s, 1H), 3.85 (qt, 1H, J = 8.2 Hz), 3.13−3.00 (m, 4H). ^{13}C NMR (400 MHz, DMSO-d_6; HCl salt) δ 160.9, 160.8, 150.3 (dd, J = 247, 9.6 Hz, F coupling), 147.9, 145.3, 140.9, 139.9, 138.2, 136.9 (dd, J = 246, 15.4 Hz, F coupling), 129.6 (d, J = 8.1 Hz), 120.8, 119.6 (dd, J = 281, 268 Hz, F coupling), 117.2, 115.2, 110.4 (d, J = 19.1 Hz), 42.2, 39.6, 20.1 (dd, J = 16.5, 5.5 Hz, 2 carbons). LRMS (ESI+)/HRMS (ESI−) m/z: calcd for $C_{19}H_{13}F_4N_5O$ 404.1, found 404.2 $[M + H]^+$/calcd 402.0978, found 402.0983 $[M - H]^-$.

4-((2-Cyclobutyl-1*H*-imidazo[4,5-*b*]pyrazin-1-yl)methyl)-8-fluoroquinolin-2(1*H*)-one (48). Compound **48** was synthesized as described for compound **47** using 4-(bromomethyl)-8-fluoroquinolin-2(1*H*)-one (**51**) and 2-cyclobutyl-1*H*-imidazo[4,5-*b*]pyrazine (**106**) as the starting materials (75% yield). HPLC: t_R = 4.98 (>98%); mp = 255.6 °C. ^{1}H NMR (400 MHz, DMSO-d_6, HCl salt) δ NH resonance not observed, 8.51 (d, 1H, J = 2.8 Hz), 8.31 (d, 1H, J = 2.8 Hz), 7.77 (d, 1H, J = 8.4 Hz), 7.51 (dd, 1H, J = 10.8, 8.4 Hz), 7.28 (m, 1H), 5.77 (s, 2H), 5.40 (s, 1H), 3.95 (qt, 1H, J = 8.0 Hz), 2.44−1.88 (m, 6H). ^{13}C NMR (DMSO-d_6) δ 162.9, 160.6, 149.0 (d, J = 245 Hz, F coupling), 147.5, 145.5 (d, J = 2.2 Hz), 140.5, 139.7, 138.0, 127.6 (d, J = 13.2 Hz), 121.8 (d, J = 6.6 Hz), 119.9 (d, J = 3.7 Hz), 118.9 (d, J = 2.9 Hz), 118.3, 116.2 (d, J = 17.6 Hz), 42.2, 31.5, 26.6 (2 carbons), 18.0. LRMS (ESI+)/HRMS (ESI−) m/z: calcd for $C_{19}H_{16}FN_5O$ 350.1, found 350.3 $[M + H]^+$/calcd 348.1261, found 348.1258 $[M - H]^-$.

8-Fluoro-4-((2-isobutyl-1*H*-imidazo[4,5-*b*]pyrazin-1-yl)methyl)-quinolin-2(1*H*)-one (49). Compound **49** was synthesized as described for compound **10** using 4-(bromomethyl)-8-fluoroquinolin-2(1*H*)-one (**51**) and 2-isobutyl-1*H*-imidazo[4,5-*b*]pyrazine (**108**) as the starting materials (25% yield). HPLC: t_R = 5.13 (>95%); mp = 250.6 °C. ^{1}H NMR (400 MHz, CD_3OD) δ 8.69 (d, 1H, J = 2.8 Hz), 8.57 (d, 1H, J = 2.8 Hz), 7.84 (d, 1H, J = 8.0 Hz), 7.51 (ddd, 1H, J = 10.4, 8.0, 0.8 Hz), 7.39 (m, 1H), 6.07 (s, 2H), 5.85 (s, 1H), 3.10 (d, 2H, J = 7.6 Hz), 2.31 (m, 1H), 1.07 (d, 6H, J = 6.8 Hz). ^{13}C NMR (400 MHz, DMSO-d_6) δ 160.6, 160.2, 149.0 (d, J = 245 Hz, F coupling), 147.7, 145.5, 140.3, 139.7, 137.9, 127.6 (d, J = 13.2 Hz), 121.8 (d, J = 7.3 Hz), 120.0 (d, J = 2.9 Hz), 118.9 (d, J = 3.0 Hz), 118.2, 116.2 (d, J = 17.6 Hz), 42.3, 35.4, 26.6, 22.2 (2 carbons). LRMS (ESI+)/HRMS (ESI−) m/z: calcd for $C_{19}H_{18}FN_5O$ 352.1, found 352.3 $[M + H]^+$/calcd 350.1417, found 350.1415 $[M - H]^-$.

4-((2-(3,3-Difluorocyclobutyl)-1*H*-imidazo[4,5-*b*]pyrazin-1-yl)-methyl)-8-fluoroquinolin-2(1*H*)-one (50). Compound **50** was synthesized as described for compound **47** using 4-(bromomethyl)-8-fluoroquinolin-2(1*H*)-one (**51**) and 2-(3,3-difluorocyclobutyl)-1*H*-imidazo[4,5-*b*]pyrazine (**110**) as the starting materials (31% yield). HPLC: t_R = 4.38 (>99%). ^{1}H NMR (400 MHz, DMSO-d_6) δ 12.08 (s, 1H), 8.54 (s, 1H), 8.35 (s, 1H), 7.75 (m, 1H), 7.39 (m, 1H), 7.28 (m, 1H), 5.80 (s, 2H), 5.42 (s, 1H), 3.85 (m, 1H), 3.16−3.01 (m, 4H). ^{13}C NMR (400 MHz, DMSO-d_6, HCl salt) δ 161.6, 161.4, 149.7 (d, J = 245 Hz, F coupling), 148.6, 146.2, 141.7, 140.6, 138.9, 128.4 (d, J = 13.2 Hz), 122.5 (d, J = 7.3 Hz), 120.8 (d, J = 3.0 Hz), 120.3 (dd, J = 282, 269 Hz, F coupling), 119.7 (d, J = 3.0 Hz), 119.0, 116.9 (d, J = 17.6 Hz), 43.1, 38.6, 20.9 (dd, J = 16.5, 5.4 Hz, 2 carbons). LRMS (ESI+)/HRMS (ESI−) m/z: calcd for $C_{19}H_{14}F_3N_5O$ 386.1, found 386.2 $[M + H]^+$/calcd 384.1072, found 384.1074 $[M - H]^-$.

***N*-(2-Fluorophenyl)-3-oxobutanamide (53).** A solution of methyl 3-oxobutanoate (54 mL, 0.5 mol) in xylene/pyridine (200 mL/5 mL) was heated to gentle reflux for 30 min. 2-Fluoroaniline (**51**, 40.0 g, 0.36 mol) was then added dropwise into the above reaction mixture, and it was refluxed for 8 h, with removal of distillate through a Dean−Stark tube. The solution was allowed to cool to 25 °C and was extracted with 20 g of NaOH in 150 mL of H_2O. The aqueous layer was separated and made weakly acidic with conc HCl. The resulting precipitate was collected by filtration, washed with H_2O, and dried to give 28 g (38%) of *N*-(2-fluorophenyl)-3-oxobutanamide (**53**) as a white crystalline solid. LRMS m/z: calcd for $C_{10}H_{10}FNO_2$ 195.0, found 196.0 $[M + H]^+$.

***N*-(2,3-Difluorophenyl)-3-oxobutanamide (54).** Compound **54** was synthesized as described for compound **53** using 3-oxobutanoate and 2,3-difluoroaniline (**52**) as starting materials (41% yield). ^{1}H NMR (400 MHz, $CDCl_3$) δ 9.52 (s, 1H), 7.99 (m, 1H), 7.04 (m, 1H), 6.89 (s, 1H), 3.64 (s, 2H), 2.33 (s, 3H). LRMS (ESI+) m/z: calcd for $C_{10}H_9F_2NO_2$ 214.0, found 214.1 $[M + H]^+$.

4-Bromo-*N*-(2-fluorophenyl)-3-oxobutanamide (55). Bromine (7.9 mL, 1.1 equiv) was added dropwise via an addition funnel to

a solution of *N*-(2-fluorophenyl)-3-oxobutanamide (**53**, 27.2 g, 0.14 mol) in AcOH (100 mL). The resulting solution was stirred at 25 °C for 5 h. Acetone (10 mL) was then added, and the solution was stirred at 25 °C for 18 h. The mixture was then concentrated to ~20% volume and worked up via EtOAc/H_2O extraction. Purification by silica gel column chromatography (10% to 20% EtOAc/hexanes) afforded 26 g (68%) of 4-bromo-*N*-(2-fluorophenyl)-3-oxobutanamide (**55**). ^{1}H NMR (400 MHz, $CDCl_3$) δ 8.77 (s, 1H), 8.23 (t, 1H, J = 8.0 Hz), 7.11 (m, 3H), 4.07 (s, 2H), 3.85 (s, 2H). LRMS m/z: calcd for $C_{10}H_9BrFNO_2$ 272.9, found 273.8 $[M + H]^+$.

4-Bromo-*N*-(2,3-difluorophenyl)-3-oxobutanamide (56). Compound **56** was synthesized as described for compound **55** using *N*-(2,3-difluorophenyl)-3-oxobutanamide (**54**) as the starting material (59% yield). ^{1}H NMR (400 MHz, $CDCl_3$) δ 8.91 (s, 1H), 8.05 (m, 1H), 7.09 (m, 1H), 6.95 (m, 1H), 4.02 (s, 2H), 3.82 (s, 2H). LRMS (ESI+) m/z: calcd for $C_{10}H_8BrF_2NO_2$ 291.9, found 292.0 $[M + H]^+$.

4-(Bromomethyl)-8-fluoroquinolin-2(1*H*)-one (57). A mixture of 4-bromo-*N*-(2-fluorophenyl)-3-oxobutanamide (**55**, 26 g, 95 mmol) and concentrated H_2SO_4 (100 mL) was heated to 45 °C for 18 h. After cooling to 25 °C, the solution was poured into ice H_2O. The solid was filtered, washed with H_2O, 10% aqueous sodium bicarbonate, and again with H_2O to give 15 g (65%) of 4-(bromomethyl)-7,8-difluoroquinolin-2(1*H*)-one (**57**) as an off-white solid. ^{1}H NMR (400 MHz, DMSO-d_6) δ 11.81 (s, 1H), 7.65 (d, 1H, J = 8.0 Hz), 7.44 (t, 1H, J = 8.1 Hz), 7.22 (m, 1H), 6.80 (s, 1H), 4.89 (s, 2H). LRMS m/z: calcd for $C_{10}H_7BrFNO$ 254.9, found 256.1 $[M + H]^+$.

4-(Bromomethyl)-7,8-difluoroquinolin-2(1*H*)-one (58). Compound **58** was synthesized as described for compound **57** using 4-bromo-*N*-(2,3-difluorophenyl)-3-oxobutanamide (**56**) as the starting material (89%). ^{1}H NMR (400 MHz, DMSO-d_6) δ 7.70 (m, 1H), 7.34 (m, 1H), 6.78 (s, 1H), 4.90 (s, 2H).

5-(1*H*-Benzo[*d*]imidazol-2-yl)-4-methylthiazole (78). Benzene-1,2-diamine (**59**, 1 g, 9.3 mmol) and 4-methylthiazole-5-carboxylic acid (**60**, 1.32 g, 9.3 mmol) were suspended in polyphosphoric acid (PPA, 20 mL) and heated to 200 °C for 4 h. The hot mixture was carefully and slowly poured into an ice/H_2O slurry with vigorous stirring. NaOH (3M) was added until a fine solid crashed out. The solid was filtered, washed with H_2O, and dried for 18 h to afford 1.2 g (60%) of 5-(1*H*-benzo[*d*]imidazol-2-yl)-4-methylthiazole (**78**) as a gray solid. ^{1}H NMR (400 MHz, DMSO-d_6) δ 12.68 (s, 1H), 9.12 (s, 1H), 7.65 (m, 1H), 7.54 (m, 1H), 7.21 (m, 2H), 2.78 (s, 3H). LRMS (ESI+) m/z: calcd for $C_{11}H_9N_3S$ 216.1, found 216.0 $[M + H]^+$.

2-Cyclobutyl-1*H*-imidazo[4,5-*b*]pyrazine (106). Compound **106** was synthesized as described for compound **78** using pyrazine-2,3-diamine (**101**) and cyclobutanecarboxylic acid (**70**) as the starting materials (heated to 100 °C) (90% yield). ^{1}H NMR (400 MHz, DMSO-d_6) δ NH resonanace not observed, 8.28 (s, 2H), 3.76 (m, 1H), 2.50−1.80 (m, 6H).

Biological Methods. Recombinant iNOS Assay (293 Transient Transfection Assay). HEK293 cells (ATCC) were seeded into 150 mm × 25 mm tissue culture plates and grown to approximately 70% confluence in DMEM containing 10% FBS, 100 U/mL penicillin, and 100 μg/mL streptomycin. Each plate was transfected with 1 mL DMEM with Pen/Strep containing 10 μg of human or murine iNOS expression plasmid and 30 μL of Fugene 6 and incubated for 4 h at 37 °C and 10% CO_2. Cells were trypsinized, resuspended to 5e5 cells/mL, and plated in 1536-well plates, followed by immediate treatment with compound. 1400W (100 μM final) was added as a positive control. After 18 h of incubation, NO production was measured by adding 2,3-diaminonaphthalene (DAN) at 10 μg/mL final concentration (Invitrogen) diluted in DMEM supplemented with hydrochloric acid (0.1 N final) and incubated for 20 min at room temperature. Fluorescence was measured after increasing pH with sodium hydroxide (0.12 N final).[26]

Recombinant eNOS and nNOS Assay (293 Transient Transfection Assays). HEK293 cells (ATCC) were seeded into 150 mm × 25 mm tissue culture plates and grown to approximately 70% confluence in DMEM containing 10% FBS, 100 U/mL penicillin, and 100 μg/mL streptomycin. Each plate was transfected with 1 mL of DMEM with Pen/Strep containing 10 μg of human or murine nNOS or 15 μg of human eNOS expression plasmid along with Fugene 6 (added in a 3:1 ratio of μL Fugene to μg plasmid) and incubated for 4 h at 37 °C and 10% CO_2. Cells were trypsinized, resuspended to 5e5 cells/mL, and plated in 384-well plates, followed by immediate treatment with compound. SEITU (100 μM final) was added as a positive control. Cells were incubated at 37 °C with 10% CO_2 for 24 h and then activated by calcium ionophore addition of either A23187 (83 nM final) for eNOS or ionomycin (30 μM final) for nNOS. After 18 h of incubation, NO production was measured as described for recombinant iNOS assay (above).

LPS Assay. A dose of 10 mg/kg of LPS (Sigma) was used in mouse endotoxemia studies. LPS was dissolved in 0.9% sodium chloride and was given as an intraperitonel injection at volume of 10 mL/kg. Male mice (Balb/c) were returned to their home cages after injection and sacrificed 6 h later. Test compounds were administered by oral gavage (prepared in 90% PEG/5% Tween 80/5% PVP + 90% CMC (0.5% w/v)) immediately before LPS injection. Blood samples were collected into EDTA containing tubes and processed for plasma collection for analysis of nitrate and drug levels. Plasma nitrate (marker of iNOS activity) levels increase gradually with peak induction achieved 6−8 h postinjection. Prior to starting the reactions, plasma samples were subjected to filtration through a 10 kDa molecular weight cutoff filter (Fisher Scientific) at 2500 rpm. Nitrates were converted to nitrites using nitrate reductase, then diaminonaphthalene (DAN) was added followed by the addition of NaOH, which converted the nitrite-DAN adduct into a fluorophore. Measurement of the fluorescence of the nitrite-DAN adduct using an Aquest plate reader (Molecular Devices) accurately determined NO_2 concentration.

Mouse Formalin Pain Model. The formalin solution for intraplantar injection was first prepared by diluting a 10% formalin solution to 5% with 0.9% saline. Test compounds were administered by oral gavage (prepared in 90% PEG/5% Tween 80/5% PVP + 90% CMC (0.5% w/v) 30 min prior to formalin injection. A volume of 20 μL of formalin solution was injected into the left hind paw of each animal. Immediately after injection of formalin into the left hind paw, the mouse was placed in a see-through observation chamber and a timer was activated. The duration of pain behaviors (hind paw flinches, licking, and biting) displayed was counted in 5 min intervals. Phase II was observed from 25 to 45 min postformalin injection. Side effects observed were also noted. Data are presented as time spent in nociceptive behaviors during phase II (25−45 min postformalin). There was a single observer throughout the study. All results are expressed as mean ± SE (n = 5−6 mice). Statistical significance is inferred from one-way analysis of variance (ANOVA) followed by appropriate post hoc analyses (GraphPad Prizm, V5.0).

Mouse Chung Model. Mice underwent a surgical procedure as described in Chung.[27] Briefly, mice were initially anesthetized with 5% isoflurane in medical-grade pure oxygen and maintained with 2−3% isoflurane during the surgical procedure. Using aseptic techniques, the left Lumbar (L) L5 and L6 spinal nerves were exposed and isolated with a surgical hook, distal to their respective dorsal root ganglion. A tight ligation was made on each nerve using a 6−0 black braided silk thread. The back muscles were sutured (6−0 braided black silk) and the skin laceration was stapled with surgical wound clips. Mice were allowed to recover from spinal nerve injury for approximately 5−10 days. The development of mechanical (tactile) allodynia was assessed using a set of calibrated von Frey filaments (Stoelting Co., IL) with increasing stiffness (0.04, 0.07, 0.16,

0.4, 1.0, 1.4, 2.0 g/force) and exerted increasing force when pushed against the tested paw for a 10 s period. The stimulation with a von Frey filament was completed within a 10 s period, and the percent response frequency was calculated using Dixon's up and down formula (Chaplan 1994). Control animals with no surgery or animals that underwent sham-surgery showed a 50% withdrawal threshold of 1.5−2 g (data not shown). Only those animals that showed baseline 50% withdrawal thresholds of ∼0.2−0.3 g anytime between 5 and 10 days postsurgery were considered to have achieved tactile allodynia and were included in all drug treatment studies.

Mouse Rotarod Assay. Effects of **42** on motor coordination were assessed in the rotarod assay.[28] Male C57Bl/6j mice were acclimated to testing room for 30 min and to rotarod device for 5 min at 4 rpm, during which animals were repeatedly returned to the device as the animals fall. Approximately 30 min post-acclimation to rotarod device, animals were subjected to two training sessions 30 min apart. Each session involved acclimation to accelerating rotarod (4−40 rpm in 300 s) with latencies to drop recorded. Only those mice with latencies of >60 s were included in the assay. Following oral administration of either gabapentin or **42**, latencies to fall on accelerating rotarod were determined at 1, 2, and 3 h postdose. Animals unable to stay on the rotarod at 4 rpm were assigned a latency of 0 s; animals completing a trial were assigned a latency of 300 s.

Acknowledgment. We thank John Walsh for high resolution mass spectra and Xing Cheng for assistance with NMR spectroscopy.

Supporting Information Available: Experimental details on the preparation of intermediates **79**−**119**, biological methods, copies of the ^{1}H NMR, ^{13}C NMR, LC trace, and high resolution mass spectra. This material is available free of charge via the Internet at http://pubs.acs.org.

References

(1) Alderton, W. K.; Cooper, C. E.; Knowles, R. G. Nitric oxide synthases: structure, function and inhibition. *Biochem. J.* **2001**, *357*, 593–615.

(2) (a) Levy, D.; Zochodne, D. W. NO Pain: Potential Roles of Nitric Oxide in Neuropathic Pain. *Pain Pract.* **2004**, *4* (1), 11–18. (b) Vallance, P.; Leiper, J. Blocking NO Synthesis: How, Where, and Why? *Nature Rev. Drug Discovery* **2002**, *1*, 939–950.

(3) Wu, J.; Fang, L.; Lin, Q.; Willis, W. D. Nitric oxide synthase in spinal cord central sensitization following intradermal injection of capsaicin. *Pain* **2001**, *94*, 47–58.

(4) Guan, Y.; Yaster, M.; Raja, S. N.; Tao, Y. Genetic knockout and pharmacologic inhibition of neuronal nitric oxide synthase attenuate nerve injury-induced mechanical hypersensitivity in mice. *Mol. Pain* **2007**, *3*, 29.

(5) Paige, J. S.; Jaffrey, S. R. Pharmacologic Manipulation of Nitric Oxide Signaling: Targeting NOS Dimerization and Protein−Protein Interactions. *Curr. Top. Med. Chem.* **2007**, *7*, 97–114.

(6) (a) Alderton, W. K.; Angell, A. D. R.; Craig, C.; Dawson, J.; Garvey, E.; Moncada, S.; Monkhouse, J.; Rees, D.; Russell, L. J.; Russell, R. J.; Schwartz, S.; Waslidge, N.; Knowles, R. G. GW274150 and GW273629 are potent and highly selective inhibitors of inducible nitric oxide synthase in vitro and in vivo. *Br. J. Pharmacol.* **2005**, *145*, 301–312. (b) Alba, D. A; Clayton, N. M.; Collins, S. D.; Colthup, P.; Chessell, I.; Knowles, R. G. GW274150, a novel and highly selective inhibitor of the inducible isoform of nitric oxide synthase (iNOS), shows analgesic effects in rat models of inflammatory and neuropathic pain. *Pain* **2006**, *120*, 170–181.

(7) Edwards, R. M.; Stack, E. J.; Trizna, W. Interaction of L-Arginine Analogs With L-Arginine Uptake in Rat Renal Brush Border Membrane Vesicles. *J. Pharmacol. Exp. Ther.* **1998**, *285*, 1019–1022.

(8) (a) LaBuda, C. J.; Koblish, M.; Tuthill, P.; Dolle, R. E.; Little, P. J. Antinociceptive activity of the selective iNOS inhibitor AR-C102222 in rodent models of inflammatory, neuropathic and post-operative pain. *Eur. J. Pain* **2005**, *10* (6), 505–512. (b) Tinker, A. C.; Beaton, H. G.; Boughton-Smith, N.; Cook, T. R.; Cooper, S. L.; Fraser-Rae, L.; Hallam, K.; Hamley, P.; McInally, T.; Nicholls, D. J.; Pimm, A. D.; Wallace, A. V. 1,2-Dihydro-4-quinazolinamines: Potent, Highly Selective Inhibitors of Inducible Nitric Oxide Synthase Which Show Antiinflammatory Activity in Vivo. *J. Med. Chem.* **2003**, *46* (6), 913–916.

(9) Davey, D. D.; Adler, M.; Arnaiz, D.; Eagen, K.; Erickson, S.; Guilford, W.; Kenrick, M.; Morrissey, M. M.; Ohlmeyer, M.; Pan, G.; Paradkar, V. M.; Parkinson, J.; Polokoff, M.; Saionz, K.; Santos, C.; Subramanyam, B.; Vergona, R.; Wei, R. G.; Whitlow, M.; Ye, B.; Zhao, Z. S.; Devlin, J. J.; Phillips, G. Design, Synthesis, and Activity of 2-Imidazol-1-ylpyrimidine Derived Inducible Nitric Oxide Synthase Dimerization Inhibitors. *J. Med. Chem.* **2007**, *50* (6), 1146–1157.

(10) Patman, J.; Bhardwaj, N.; Ramnauth, J.; Annedi, S. C.; Renton, P.; Maddaford, S. P.; Rakhit, S.; Andrews, J. S. Novel 2-aminobenzothiazoles as selective neuronal nitric oxide synthase inhibitors. *Bioorg. Med. Chem. Lett.* **2007**, *17*, 2540–2544.

(11) Nason, D. M.; Heck, S. D.; Bodenstein, M. S.; Lowe, J. A., III; Nelson, R. B.; Liston, D. R.; Nolan, C. E.; Lanyon, L. F.; Ward, K. M.; Volkmann, R. A. Substituted 6-phenyl-pyridin-2-ylamines: selective and potent inhibitors of neuronal nitric oxide synthase. *Bioorg. Med. Chem. Lett.* **2004**, *14*, 4511–4514.

(12) Bonnefous, C.; Payne, J. E.; Roppe, J.; Zhang, H.; Chen, X.; Symons, K. T.; Nguyen, P. H.; Sablad, M.; Rozenkrants, N.; Zhang, Y.; Wang, L.; Severance, D.; Walsh, J. P.; Yazdani, N.; Shiau, A. K.; Noble, S. A.; Rix, P.; Rao, T. S.; Hassig, C. A.; Smith, N. D. Discovery of Inducible Nitric Oxide Synthase (iNOS) Inhibitor Development Candidate KD7332, Part 1: Identification of a Novel, Potent, and Selective Series of Quinolinone iNOS Dimerization Inhibitors That Are Orally Active in Rodent Pain Models. *J. Med. Chem.* **2009**, *52* (9), 3047–3062.

(13) As disclosed previously, modification of the quinolinone portion of **8** did not lead to an improvement in rodent pharmacokinetics. See ref 11.

(14) Choi, H. Y.; Chi, D. Y. Nonselective Bromination-Selective Debromination Strategy: Selective Bromination of Unsymmetrical Ketones on Singly Activated Carbon against Doubly Activated Carbon. *Org. Lett.* **2003**, *5* (4), 411–414.

(15) Later in the project, we found higher yields could be obtained by alkylating the benzimidazole core with **58** by heating the two starting materials neat under a N_2 atmosphere (see preparation of compound **47**).

(16) The regioselectivity of the desired compound **42** was confirmed by the characteristic shift of the quinolinone C3 hydrogen (DMSO-d_6: δ = 5.36 (s, 1H)) compared to the undesired regiosiomer **43** (DMSO-d_6: δ = 6.26 (s, 1H)). A similar shift was seen for compound **25** (DMSO-d_6: δ = 5.53 (s, 1H)), the structure of which was confirmed by X-ray Diffraction. Similar chemical shifts of the quinolinone C3 hydrogen were observed with analogues **33**−**41**, **44**−**50**.

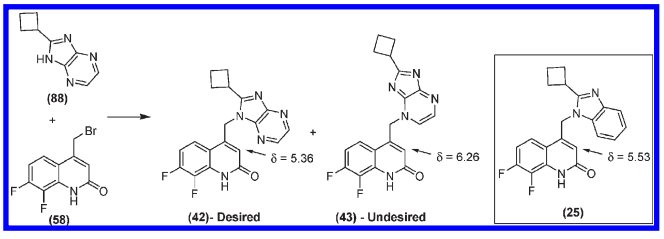

(17) Elimination rate under conditions of combined phase I oxidation and phase II glucoronide conjugation.

(18) Alkylation of the symmetrical benzimidazole core can lead only to the desired compound **42** and the region-isomer **43**. In contrast, alkylation of the nonsymmetrical benzimidazoles to give compounds **36**−**41** can lead to three products.

(19) Wang, L. X.; Wang, Z. J. Animal and cellular models of chronic pain. *Adv. Drug Delivery Rev.* **2003**, *55*, 949–965.

(20) Dubuisson, D.; Dennis, S. G. The Formalin Test: A Quantitative Study of the Analgesic Effects of Morphine, Meperidine, and Brain Stem Stimulation in Rats and Cats. *Pain* **1977**, *4*, 161–174.

(21) The brain penetration of **42** was determined in the rat by microdialysis and was found to be 2% of the plasma concentration (see ref 22).

(22) Symons, K. T.; Nguyen, P. H.; Massari, M. E.; Anzola, J. V.; Staszewski1, L. M.; Wang, L.; Yazdani, N.; Dorow, S.; Muhammad, J.; Sablad, M.; Rozenkrants, N.; Bonefous, C.; Payne, J. E.; Rix, P.;

Shiau, A. K.; Noble, S. A.; Smith, N. D.; Hassig, C. A.; Zhang, Z.; Rao, T. S. *J. Pharmacol. Exp. Ther.*, **2010**, in press.
(23) De Laeter, J. R. Atomic Weights of the Elements. *Pure Appl. Chem.* **1991**, *63* (7), 975–90.
(24) Singh, M. P.; Bathini, Y.; Lown, J. W. Site Selective Alkoxymethylation of Imidazo[4,5-*b*]pyridines: Structural Analysis by High Field NMR Methods. *Heterocycles* **1993**, *36* (5), 971–985.
(25) See Supporting Information for NOE traces and for compound numbering.
(26) Misko, T. P.; Schilling, R. J.; Salvemini, D.; Moore, W. M.; Currie, M. G. A fluorometric assay for the measurement of nitrite in biological samples. *Anal. Biochem.* **1993**, *214*, 11–16.
(27) Kim, S. H.; Chung, J. M. An experimental model for peripheral neuropathy produced by segmental spinal nerve ligation in the rat. *Pain* **1992**, *50*, 355–363.
(28) Dunham, N. W.; Miya, T. S. A note on a simple apparatus for detecting neurological deficit in rats and mice. *J. Am. Pharm. Assoc.* **1957**, *46*, 208–209.